

ANTICANCER EFFECTS OF MANSONONE G DERIVATIVE ON HUMAN COLORECTAL
CANCER CELLS



A Thesis Submitted in Partial Fulfillment of the Requirements
for the Degree of Master of Science in Pharmacology
Inter-Department of Pharmacology
Graduate School
Chulalongkorn University
Academic Year 2018
Copyright of Chulalongkorn University

ฤทธิ์ต้านมะเร็งของสารอนุพันธ์ของ mansonone G ต่อเซลล์มะเร็งลำไส้ใหญ่และไส้ตรงของมนุษย์



วิทยานิพนธ์นี้เป็นส่วนหนึ่งของการศึกษาตามหลักสูตรปริญญาวิทยาศาสตรมหาบัณฑิต

สาขาวิชาเภสัชวิทยา สหสาขาวิชาเภสัชวิทยา

บัณฑิตวิทยาลัย จุฬาลงกรณ์มหาวิทยาลัย

ปีการศึกษา 2561

ลิขสิทธิ์ของจุฬาลงกรณ์มหาวิทยาลัย

สาวิณี จันทรวิจิตร : ฤทธิ์ต้านมะเร็งของสารอนุพันธ์ของ mansonone G ต่อเซลล์มะเร็งลำไส้ใหญ่และไส้ตรงของมนุษย์. (

ANTICANCER EFFECTS OF MANSONONE G DERIVATIVE ON HUMAN COLORECTAL CANCER CELLS) อ.ที่ปรึกษาหลัก : ผศ.ดร.ปิยนุช วงศ์อนันต์, อ.ที่ปรึกษาร่วม : รศ.จันทน์ อธิพานิชพงศ์

Mansonone G (MG) เป็นสารในกลุ่ม 1,2-naphthoquinone ซึ่งสกัดได้จากเนื้อไม้ของต้น *Mansonia gagei* Drumm (ต้นจันทน์ขม) มีฤทธิ์ทางเภสัชวิทยาที่หลากหลาย เช่น ฤทธิ์ต้านแบคทีเรีย ฤทธิ์ต้านฮอร์โมนเอสโตรเจน และฤทธิ์ต้านเซลล์ไขมัน แต่ยังไม่เคยมีรายงานเกี่ยวกับฤทธิ์ต้านมะเร็งของสาร MG และสารอนุพันธ์ของ MG ทั้งหมด 10 ชนิดต่อเซลล์มะเร็งลำไส้ใหญ่และไส้ตรง ดังนั้นวัตถุประสงค์ของงานวิจัยนี้คือ เพื่อศึกษาความเป็นพิษของสาร MG และสารอนุพันธ์ของ MG ทั้งหมด 10 ชนิดและกลไกการออกฤทธิ์ของสารที่มีความเป็นพิษที่สุดต่อเซลล์มะเร็งลำไส้ใหญ่และไส้ตรงสองชนิด ได้แก่ HCT-116 ซึ่งเป็นเซลล์ที่มี p53 ปกติ และ HT-29 ซึ่งเป็นเซลล์ที่มี p53 กลายพันธุ์ ผลการศึกษาพบว่าสาร MG และสารอนุพันธ์ MG สามารถยับยั้งการอยู่รอดของเซลล์ HCT-116 และเซลล์ HT-29 แบบขึ้นอยู่กับความเข้มข้น และจากการทดสอบกับสารทุกตัวพบว่า G07 มีความเป็นพิษต่อเซลล์มะเร็งลำไส้ใหญ่และไส้ตรงมากที่สุดและมีความเป็นพิษน้อยต่อเซลล์ปกติ ได้แก่ PCS201-010 และ CRL-1790 การศึกษาในระดับกลไกพบว่า G07 สามารถเหนี่ยวนำให้เซลล์ HCT-116 และเซลล์ HT-29 เกิดการตายแบบอะพอพโทซิสผ่านการสร้างอนุมูลอิสระและ *N-acetyl cysteine* (NAC) สามารถลดผลของ G07 ต่อการตายแบบอะพอพโทซิสของเซลล์ HCT-116 และเซลล์ HT-29 การทดสอบด้วยวิธี western blot แสดงให้เห็นว่า G07 ลดการแสดงออกของโปรตีน Bcl-2 and Bcl-xl ในเซลล์ทั้งสองชนิดและเพิ่มการแสดงออกของโปรตีน Bak ในเซลล์ HT-29 นอกจากนี้ G07 ยังสามารถลดการทำงานของวิถีสัญญาณ AKT และปรับเปลี่ยนวิถีสัญญาณ ERK1/2 โดยยับยั้งการเติมหมู่ฟอสเฟตของ ERK1/2 ในเซลล์ HCT-116 และกระตุ้นการเติมหมู่ฟอสเฟตของ ERK1/2 ในเซลล์ HT-29 โดยสรุปผลการศึกษาี้แสดงให้เห็นฤทธิ์ต้านมะเร็งของ G07 ต่อเซลล์มะเร็งลำไส้ใหญ่และไส้ตรงของมนุษย์โดยการเหนี่ยวนำให้เซลล์เกิดการตายแบบอะพอพโทซิส การสร้างอนุมูลอิสระและปรับเปลี่ยนวิถีสัญญาณ ERK1/2 และ AKT ซึ่งผลการศึกษาี้ทำให้เห็นว่า G07 เป็นสารที่สามารถพัฒนาเป็นสารต้านมะเร็งที่ใช้ในการรักษาโรคมะเร็งลำไส้ใหญ่และไส้ตรง

สาขาวิชา เภสัชวิทยา

ปีการศึกษา 2561

ลายมือชื่อนิสิต

ลายมือชื่อ อ.ที่ปรึกษาหลัก

ลายมือชื่อ อ.ที่ปรึกษาร่วม

5887268420 : MAJOR PHARMACOLOGY

KEYWORD: Mansonone G, Colorectal cancer, Cytotoxicity, Apoptosis, ROS, Anticancer effect

Savinee Chanvijit :
 ANTICANCER EFFECTS OF MANSONONE G DERIVATIVE ON HUMAN COLORECTAL CAN
 CER CELLS. Advisor: Asst. Prof. PIYANUCH WONGANAN, Ph.D. Co-advisor: Assoc. Prof.
 Chandhanee Itthipanichpong

Mansonone G (MG), 1,2-naphthoquinone, isolated from the heartwood of *Mansonia gagei* Drumm (Chan-Cha-Mod), exhibited several pharmacological effects including anti-bacterial, anti-estrogenic and anti-adipogenic effects. However, anticancer activity of MG and its derivatives on colorectal cancer (CRC) has never been investigated. Therefore, the objective of this study was to investigate the cytotoxic effect of MG and its derivatives and to determine the mechanism(s) underlying cytotoxicity of the most potent MG derivative on two CRC cell lines, HCT-116 cells carrying p53 wild-type and HT-29 cells carrying p53 mutant. In the present study, MG and its derivatives could inhibit viability of HCT-116 and HT-29 cells in a concentration-dependent manner. Of all MG and its derivatives, G07 was the most potent cytotoxic agent toward the cancer cells and less toxic to normal cells, PCS201-010 and CRL-1790. Mechanistic studies revealed that G07 could induce apoptosis through ROS generation in both HCT-116 and HT-29 cells and this effect was abolished by *N*-acetyl cysteine (NAC). Western blot analysis revealed that G07 downregulated the expression of Bcl-2 and Bcl-xl proteins in both cells and upregulated the expression of Bak protein in HT-29 cells. Moreover, G07 downregulated AKT signaling pathway and modulated ERK1/2 signaling pathway by inhibiting ERK1/2 phosphorylation in HCT-116 cells and activating ERK1/2 phosphorylation in HT-29 cells. Taken together, the present study demonstrated that G07 exerted a potent anticancer effect toward human colorectal cancer cells which was associated with induction of apoptosis, generation of ROS and modulation of ERK1/2 and AKT signaling pathways, suggesting that G07 is a promising compound for further development as an anticancer agent in CRC treatment.

Field of Study: Pharmacology

Student's Signature

Academic Year: 2018

Advisor's Signature

Co-advisor's Signature

ACKNOWLEDGEMENTS

I have been accompanied and supported by many people. Without their passionate participation and help, this research project could not have been successfully completed. Firstly, I would like to express my sincere gratitude to my advisor, Assistant Professor Dr. Piyanuch Wonganan, and my thesis co-advisor, Associated Professor Chandanee Itthipanichpong, at the Department of Pharmacology, Faculty of Medicine for their continuous support throughout my master's degree study. Thank you for their patience, motivation, and attention. Their guidance helped me in all the time of researching and writing of this thesis. I could not have imagined having a better advisor and mentor of my master's degree study.

I would like to gratefully acknowledge the experts who were involved in this research project: Assistant Professor Dr. Warinthorn Chavasiri, Department of Chemistry, Faculty of Science, Chulalongkorn University for providing MG and its derivatives. Associated Professor Dr. Amornpun Sereemaspen, Department of Anatomy, Faculty of Medicine, Chulalongkorn University for providing normal colon cells, CRL-1790. Nalinee Pradubyat, Department of Pharmacology, Faculty of Pharmacy, Rangsit University for providing primary dermal fibroblasts cells, PCS201-010. Dr. Supranee Buranapraditkun, Allergy and Clinical Immunology Unit, Department of Medicine, Faculty of Medicine, Chulalongkorn University for technical assistance on flow cytometry.

This research has been financially supported by 90th Anniversary of Chulalongkorn University Fund (Ratchadaphiseksompot Endowment Fund), grant no. GCUGR1125612040M (S.C.).

I would also like to thank you all Ph.D. and master's students in the Cell Culture Laboratory at the Department of Pharmacology, Faculty of Medicine for supporting, training all basic cell culture techniques, and especially their friendship. I really enjoyed the happy moments spent with them.

Finally, I must express my very profound gratitude to my family for providing me with unfailing support and continuous encouragement throughout my years of study

and through the process of researching and writing this thesis. This accomplishment would not have been possible without them. Thank you.

Savinee Chanvijit



TABLE OF CONTENTS

	Page
ABSTRACT (THAI).....	iii
ABSTRACT (ENGLISH).....	iv
ACKNOWLEDGEMENTS.....	v
TABLE OF CONTENTS.....	vii
LIST OF TABLES.....	x
LIST OF FIGURES.....	xi
LIST OF ABBREVIATIONS.....	xiii
CHAPTER I INTRODUCTION.....	1
1.1 Background and rationale.....	1
1.2 Objectives.....	3
1.3 Hypothesis.....	3
CHAPTER II LITERATURE REVIEWS.....	4
2.1 Colorectal cancer.....	4
2.1.1 Risk factors of CRC.....	6
2.1.2 Symptoms of CRC.....	8
2.1.3 Stages of CRC.....	8
2.1.4 Treatment of CRC.....	9
2.2 Reactive Oxygen Species.....	11
2.3 Apoptosis.....	12
2.3.1 Death-receptor-induced extrinsic apoptotic pathway.....	13
2.3.2 Mitochondrial-apoptosome-mediated intrinsic apoptotic pathway.....	14

2.4 MAPK Signaling pathway	15
2.5 PI3K/AKT signaling pathway.....	16
2.6 Mansonone G and its derivatives.....	17
CHAPTER III MATERIALS AND METHODS	23
3.1 Equipment	23
3.2 Materials.....	23
3.3 Reagents.....	24
3.4 Methods	26
3.4.1 Cell culture	26
3.4.2 Preparation of mansonone G and its derivatives stock solution	26
3.4.3 Determination of cell viability by MTT assay.....	26
3.4.4 Analysis of apoptosis using Annexin V-FITC/PI staining.....	27
3.4.5 Evaluation of protein expression using western blot analysis	28
3.4.6 Determination of intracellular ROS using DCFH-DA assay	29
3.4.7 Statistical analysis	29
CHAPTER IV RESULTS	30
4.1 Effect of mansonone G and mansonone G derivatives on the viability of colorectal cancer cells	30
4.2 Effects of mansonone G derivatives on the viability of normal cells	33
4.3 Effect of G07 on the viability of HCT-116 cells.....	35
4.4 Effect of G07 on apoptotic cell death in HCT-116 cells.....	36
4.5 Effect of G07 on the expression of Bcl-2 family proteins in HCT-116 cells.....	38
4.6 Effect of G07 on ROS generation in HCT-116 cells	40
4.7 Generation of ROS mediates G07-induced apoptosis in HCT-116 cells.....	43

4.8 Effect of G07 on MAPK and PI3K/AKT signaling pathways in HCT-116 cells	44
4.9 Effect of G07 on viability of HT-29 cells.....	47
4.10 Effect of G07 on apoptotic cell death in HT-29 cells	48
4.11 Effect of G07 on expression of Bcl-2 family proteins in HT-29 cells.....	51
4.12 Effect of G07 on ROS generation in HT-29 cells.....	54
4.13 Generation of ROS mediates G07-induced apoptosis in HT-29 cells.....	56
4.14 Effect of G07 on MAPK and PI3K/AKT signaling pathways in HT-29 cells.....	57
CHAPTER V DISCUSSION AND CONCLUSION.....	59
REFERENCES	65
APPENDIX A PREPARATION OF REAGENTS	75
APPENDIX B RESULTS.....	80
VITA.....	85

LIST OF TABLES

Page

Table 1: IC ₅₀ values of MG and its derivatives on HCT-116 and HT-29 cells	33
--	----



LIST OF FIGURES

	Page
Figure 1 Anatomy of the large intestine	5
Figure 2 The number of new cancer patients of colorectal cancer	5
Figure 3 The number of deaths of colorectal cancer	6
Figure 4 The colorectal adenoma-carcinoma sequence	7
Figure 5 Intrinsic and extrinsic apoptosis pathways.....	13
Figure 6 Bcl-2 family proteins.....	15
Figure 7 ERK1/2 MAPK signaling pathway	16
Figure 8 PI3K/AKT signaling pathway	17
Figure 9 Structure of mansonone G.....	18
Figure 10 Structures of mansonone G derivatives.....	22
Figure 11 Effects of MG and its derivatives (G01-G04) on the viability of HCT-116 and HT-29 cells.	31
Figure 12 Effects of mansonone G derivatives (G05-G10) on the viability of HCT-116 and HT-29 cells.	32
Figure 13 Effects of G03, G04, G07 and G10 on the viability of PCS201-010 cells.....	34
Figure 14 Effects of G07 on the viability of CRL-1790 cells.....	35
Figure 15 Effect of G07 on the viability of HCT-116 cells.	36
Figure 16 Effect of G07 on apoptosis in HCT-116 cells.	37
Figure 17 Effect of G07 on PARP cleavage in HCT-116 cells.	38
Figure 18 Effect of G07 on the expression of pro-apoptotic Bcl-2 family proteins in HCT-116 cells.....	39
Figure 19 Effect of G07 on the expression of anti-apoptotic Bcl-2 family proteins in HCT-116 cells.....	40


Figure 20 Effect of G07 on ROS generation in HCT-116 cells.....	42
Figure 21 Effect of ROS in G07-induced apoptosis in HCT-116 cells.	44
Figure 22 Effect of G07 on the expression of ERK1/2 and PI3K/AKT signaling proteins in HCT-116 cells.....	46
Figure 23 Effect of G07 on the viability of HT-29 cells.....	48
Figure 24 Effect of G07 on apoptosis in HT-29 cells.....	49
Figure 25 Effect of G07 on PARP cleavage in HT-29 cells.....	50
Figure 26 Effect of G07 on the expression of pro-apoptotic Bcl-2 family proteins in HT-29 cells.....	52
Figure 27 Effect of G07 on the expression of anti-apoptotic Bcl-2 family proteins in HT-29 cells.....	53
Figure 28 Effect of G07 on ROS generation of HT-29 cells.....	55
Figure 29 Effect of ROS on G07-induced apoptosis in HT-29 cells.....	56
Figure 30 Effect of G07 on the expression of ERK1/2 and PI3K/AKT signaling proteins in HT-29 cells.....	58

LIST OF ABBREVIATIONS

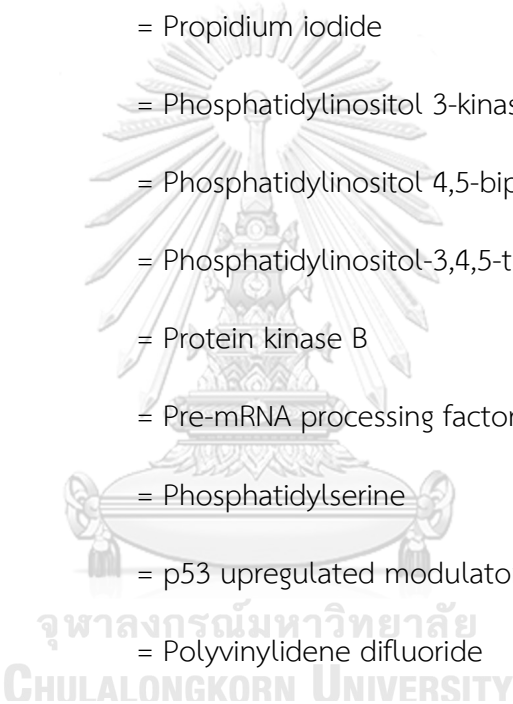
%	= Percentage
µg	= Microgram
µg/ml	= Microgram per milliliter
µl	= Microliter
µM	= Micromolar
5-FU	= 5-fluorouracil
AIF	= Apoptosis-inducing factor
AJCC	= American Joint Committee on Cancer
ANOVA	= Analysis of variance
Apaf-1	= Apoptosis protein-activating factor 1
APC	= Adenomatous polyposis coli
ATCC	= American Type Culture Collection
ATP	= Adenosine triphosphate
Bak	= Bcl-2 homologous antagonist killer
Bax	= Bcl-2 associated X protein
Bcl-2	= B-cell lymphoma-2
Bcl-xl	= B-cell lymphoma-extra large
BH domain	= Bcl-2 homology domain
Caspase	= Cysteine aspartic acid specific protease
CD	= Cluster of differentiation
CO ₂	= Carbon dioxide
cPARP	= Cleaved poly (ADP-ribose) polymerase

CRC	= Colorectal cancer
DCF	= 2',7'-dichlorofluorescein
DCFH-DA	= 2',7'-dichloro-dihydro-fluorescein diacetate
DIABLO	= Direct inhibitor of apoptosis-binding protein with a low iso-electric point
DISC	= Death-inducing signaling complex
DMEM	= Dulbecco's Modified Eagle Medium
DMSO	= Dimethyl sulfoxide
DNA	= Deoxyribonucleic acid
DR	= Death receptor
EDTA	= Ethylene diamine tetraacetic acid
EGF	= Epidermal growth factor
EGFR	= Epidermal growth factor receptor
Endo G	= Endonuclease G
ER	= Estrogen receptor
ERK	= Extracellular signal-regulated kinase
FAP	= Familial adenomatous polyposis
FasR	= Fibroblast associated antigen receptor
FBS	= Fetal bovine serum
FdUMP	= Fluorodeoxyuridine monophosphate
FdUTP	= Fluorodeoxyuridine triphosphate
FITC	= Fluorescein isothiocyanate

FNQ	= Furano-1,2-naphthoquinone
FUTP	= Fluorouridine triphosphate
g/mol	= Gram per mole
GAPDH	= Glyceraldehyde 3-phosphate dehydrogenase
GDP	= Guanosine diphosphate
GEF	= Guanine nucleotide exchange factor
Grb2	= Growth factor receptor-bound protein 2
GTP	= Guanosine-5'-triphosphate
h	= Hour
H ₂ O ₂	= Hydrogen peroxide
HBSS	= Hank's buffered salt solution
HNPCC	= Hereditary nonpolyposis colorectal cancer
HRP	= Horseradish peroxidase
IARC	= International Agency for Research on Cancer
IC ₅₀	= The half maximal inhibitory concentration
JNK	= c-Jun N-terminal kinase
KIT	= Stem cell factor receptor
KRAS	= Kirsten rat sarcoma viral oncogene homolog
LSD	= Least square difference
MAPK	= Mitogen-activated protein kinase
MBC	= Minimum bactericidal concentration
MEK	= Mitogen-activated protein kinase



MG	= Mansonone G
MIC	= Minimum inhibitory concentration
ml	= Milliliter
mM	= Millimolar
MOMP	= Mitochondria outer membrane permeabilization
mRNA	= Messenger ribonucleic acid
mTOR	= Mammalian target of rapamycin
MTT	= 3-(4, 5-dimethylthiazol-2-yl)-2,5-diphenyltetrazolium bromide
MW	= Molecular weight
NAC	= <i>N</i> -acetyl cysteine
NaOH	= Sodium hydroxide
NCI	= National Cancer Institute
NFDM	= Non-fat dry milk
NLEM	= National List of Essential Medicine
nm	= Nanometer
NRAS	= Neuroblastoma rat sarcoma viral oncogene homolog
O ₂ ⁻	= Superoxide anion
OH•	= Hydroxyl radicals
p53	= Tumor suppressor protein 53
PAGE	= Polyacrylamide gel electrophoresis
p-AKT	= Phosphorylated protein kinase B
PARP	= Poly (ADP-ribose) polymerase



PBS	= Phosphate buffer saline
PDGFR	= Platelet-derived growth factor receptor
PDK1	= Phosphoinositide-dependent kinase 1
PEITC	= Phenethyl isothiocyanate
p-ERK	= Phosphorylated- extracellular signal-regulated kinases
PH domain	= Pleckstrin homology domain
PI	= Propidium iodide
PI3K	= Phosphatidylinositol 3-kinase
PIP2	= Phosphatidylinositol 4,5-biphosphate
PIP3	= Phosphatidylinositol-3,4,5-triphosphate
PKB (AKT)	= Protein kinase B
Prp4B	= Pre-mRNA processing factor 4B
PS	= Phosphatidylserine
PUMA	= p53 upregulated modulator of apoptosis
PVDF	= Polyvinylidene difluoride
RAF	= Rapidly accelerated fibrosarcoma
RAS	= Rat sarcoma viral oncogene homolog
RIPA	= Radioimmunoprecipitation assay
ROS	= Reactive oxygen species
RPM	= Revolutions per minute
RPMI	= Roswell Park Memorial Institute
SDS	= Sodium dodecyl sulfates

SEM	= Standard error of mean
Smac	= Second mitochondria-derived activator of caspases
Sos	= Son of sevenless
SPSS	= Statistical package for the social sciences
TEMED	= Tetramethylethylenedimine
TKIs	= Tyrosine kinase inhibitors
TLC	= Thin-layer chromatography
TNFR	= Tumor necrosis factor receptor
TPA	= 12- <i>O</i> -tetradecanoylphorbol-13-acetate
TRAILR	= TNF-related apoptosis-inducing ligand receptor
TS	= Thymidylate synthase
UV	= Ultraviolet irradiation
VEGF	= Vascular endothelial growth factor
XIAP	= X-linked inhibitor of apoptosis protein

CHAPTER I

INTRODUCTION

1.1 Background and rationale

Colorectal cancer (CRC) is one of the most common cancer worldwide. In 2018, the International Agency for Research on Cancer (IARC) revealed that colorectal cancer was the third most common cancer in the world and there were 1,849,518 new colorectal cancer cases and 880,792 colorectal cancer deaths (1). In Thailand, the National Cancer Institute (NCI) reported that CRC is the third most commonly diagnosed in men and women (2). Treatment options of CRC are surgery, radiotherapy, chemotherapy and targeted therapy. The drugs commonly used in CRC are 5-fluorouracil (5-FU), oxaliplatin and irinotecan (3, 4). Although chemotherapy has been widely used, several side effects have hampered its application. Moreover, acquired drug resistance also limits the effectiveness of chemotherapy. Therefore, new compounds with potent anticancer activity are urgently needed.

Reactive oxygen species (ROS) such as superoxide anion (O_2^-), hydrogen peroxide (H_2O_2) and hydroxyl radicals (OH^\bullet), are involved in cell signaling, cellular senescence, cell cycle arrest and apoptosis (5-10). Increased ROS level can damage cellular components such as lipids, proteins and nucleic acids (11-13). Cancer cells frequently exhibit higher level of ROS compared with normal cells which can assist cell survival and cell proliferation. However, excessive production of ROS can also induce oxidative stress-mediated apoptosis in cancer cells (10). It was reported that many chemotherapeutic agents such as doxorubicin, vinblastine, camptothecin and cisplatin exhibited anticancer activity through increased ROS, resulting in DNA damage (14, 15). Thereby, generation of ROS might be an effective strategy for cancer treatment.

Apoptosis, a programmed cell death, is important for maintaining homeostasis of multicellular organisms. Dysregulation of apoptosis is considered one of the hallmarks of cancer and contributes to anticancer drug resistance (16). It is known that anti-apoptotic proteins are frequently upregulated and pro-apoptotic proteins are often downregulated in solid tumors (16, 17). In addition, most chemotherapeutic agents promote cells to undergo apoptosis by modulating expression and function of pro- and anti-apoptotic proteins (18, 19).

Previous studies reported that mansonone, a 1,2-naphthoquinone, has several pharmacological effects including anti-bacterial, anti-fungal, anti-estrogenic, anti-oxidant, anti-adipogenic and anti-cancer effects (20-22). Wang D et al. showed that mansonone E and F, isolated from *Ulmus pumila*, displayed anticancer activity against many types of cancer, including melanoma (A375-S2), cervical cancer (HeLa), breast cancer (MCF-7) and lymphoma (U937). Mansonone E could induce apoptosis in HeLa cells by breaking oligonucleosome, activating caspase-3, decreasing the expression of anti-apoptotic proteins, Bcl-2 and Bcl-xL, and increasing the expression of a pro-apoptotic protein, Bax (23). Similarly, mansonone E, isolated from *Thespesia populnea*, exhibited anticancer effect in several types of cancer including breast cancer (MCF-7), cervical cancer (HeLa), colorectal cancer (HT-29) and oral cavity cancer (KB) and its IC₅₀ values were 0.05, 0.55, 0.18 and 0.4 μ M, respectively (24). Furthermore, toxicity of mansonone E, extracted from the root bark of *Ulmus davidiana*, against various human leukemia cell lines, including HL60, K562, THP-1 and U937 has been found (25).

Recently, Hairani et al. has reported that mansonone G (MG), a major product extracted from the heartwood of *Mansonia gagei* Drumm, had anti-bacterial activity. Notably, increasing alkyl chain length of ether analogues of MG resulted in higher antibacterial activity (20). However, anticancer activity of MG and its derivatives on colorectal cancer cells has never been investigated. Therefore, the present study

aimed to determine the cytotoxicity of MG and its derivatives on two colorectal cancer cells lines, p53-wild-type HCT-116 cells and p53-mutant HT-29 cells.

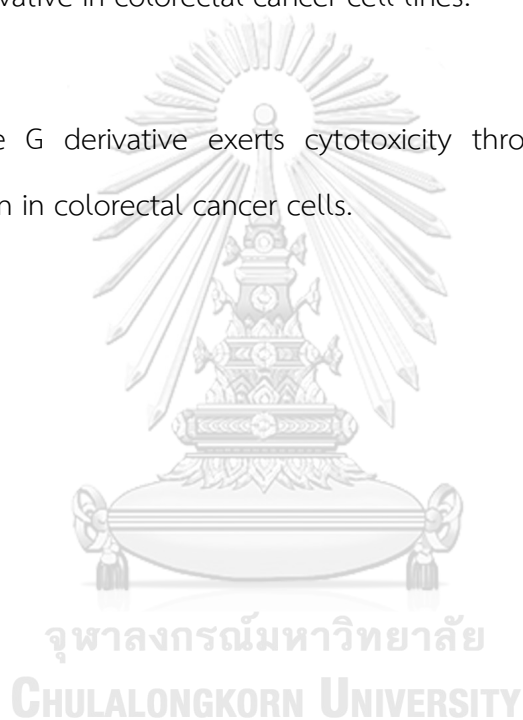
1.2 Objectives

To investigate the cytotoxic effects of mansonone G and its derivatives on two colorectal cancer cell lines, p53-wild-type HCT-116 cells and p53-mutant HT-29 cells.

To determine the mechanism(s) underlying cytotoxicity of the most potent mansonone G derivative in colorectal cancer cell lines.

1.3 Hypothesis

Mansonone G derivative exerts cytotoxicity through ROS generation and apoptosis induction in colorectal cancer cells.



CHAPTER II

LITERATURE REVIEWS

2.1 Colorectal cancer

Colorectal cancer (CRC) develops in the cells lining inside the colon or rectum (Figure 1). Among many types of cancer, incidence and mortality rate of CRC remain high. In 2018, the International Agency for Research on Cancer (IARC) revealed that CRC is the third most common cancer among men and women in the world (Figure 2) and is the second leading cause of death (Figure 3) (1). In the United States, the American Cancer Society reported that CRC is the third leading cause of cancer-related death in 2017 (26). An estimated 135,430 new cases were diagnosed with CRC while the mortality was 50,260 deaths from the disease (27). In Thailand, the National Cancer Institute (NCI) reported that CRC has been the third most common newly cancer patient for many years. The incidence rates of CRC in 2016 were 14.83% and 8.77% of all cases in men and women, respectively and estimated percentages of new cancer patients with stage I, II, III and IV were 3.69%, 15.27%, 34.98% and 38.18%, respectively of all patients (2).

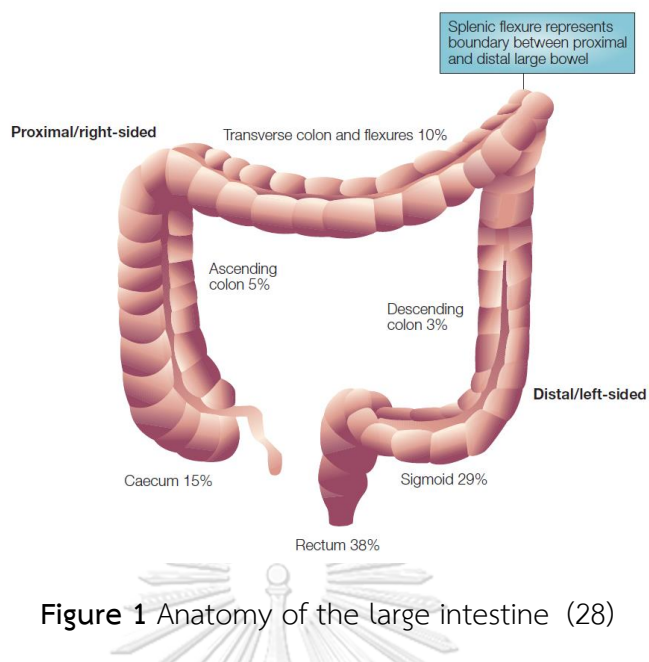


Figure 1 Anatomy of the large intestine (28)

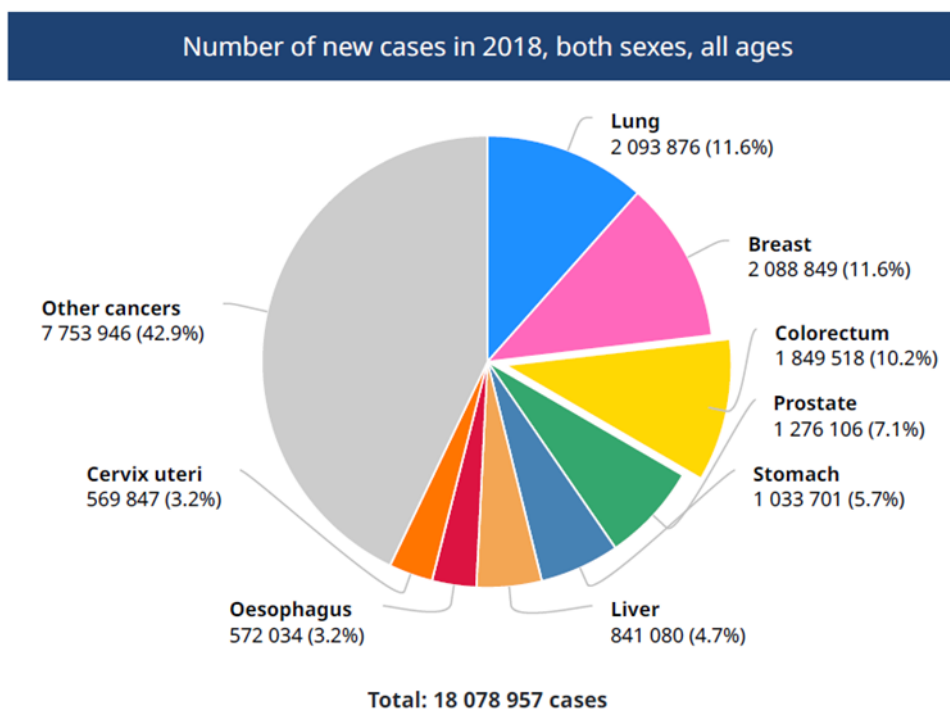


Figure 2 The number of new cancer patients of colorectal cancer (1)

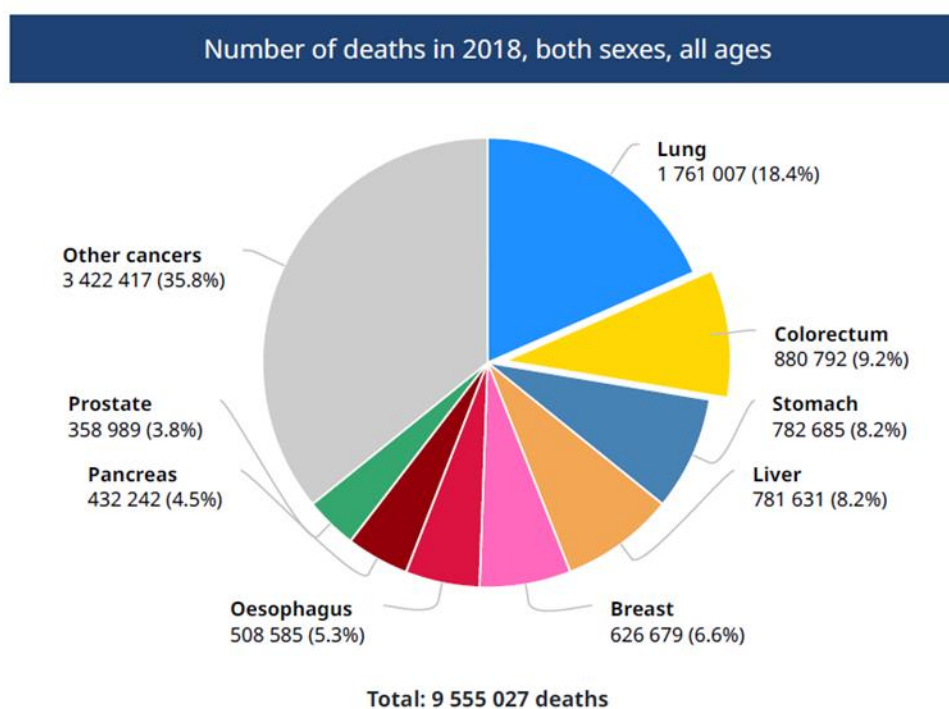


Figure 3 The number of deaths of colorectal cancer (1)

2.1.1 Risk factors of CRC

Many factors including age, family history, genetic alteration, personal disease history, diet and lifestyle can increase the risk of CRC. More than 90% of CRC patients are older than 50 years old, with the average age at diagnosis is 64 years old (29). CRC cases can be classified into 3 groups including sporadic, familial and inherited. Most of the CRC is sporadic. Approximately 70-80% of CRC patients have no family history while approximately 15-20% of cases occur in patient who have family history of CRC. The common forms of inherited CRC are familial adenomatous polyposis (FAP) and hereditary nonpolyposis colorectal cancer (HNPCC), accounting for 5-10% of all CRC. Most patients with familial and inherited CRC develop very large number of adenomas and subsequent CRC at a young age. Additionally, personal disease history, including inflammatory bowel disease, ulcerative colitis, Crohn's disease and history of polyp, also increases the risk of CRC (29-32). Genetic alterations also increase the risk of CRC. The accumulation of the mutations in specific genes such as adenomatous polyposis

coli (APC), Kirsten-RAS (KRAS) and p53 drives the transition from normal epithelium through adenoma and subsequent CRC (33). APC is the most common mutated gene in familial, inherited and sporadic CRC. Activation of KRAS, a member of MAPK pathway, also play a critical role in the progression of CRC. Mutated KRAS has been detected in 40% of sporadic CRC (34). In addition, p53 is the most common mutated gene in human cancer and its mutation occurs approximately 50% of CRC (35-37). Loss of p53 is associated with a progression from late adenoma to carcinoma and patients with mutant p53 are more resistant to chemotherapy than patients with wild-type p53 (38). It was reported that patients with p53 mutations are likely to have poor prognosis and less response to 5-FU (39). Moreover, both dietary and lifestyle also affect the development of CRC. It is shown that dietary such as high consumption of red meat and unsaturated fat is associated with an increased risk of CRC. Similarly, people with excessive alcohol consumption and long-term cigarette smoking have an increased risk of CRC more than people who do not consume the products (40).

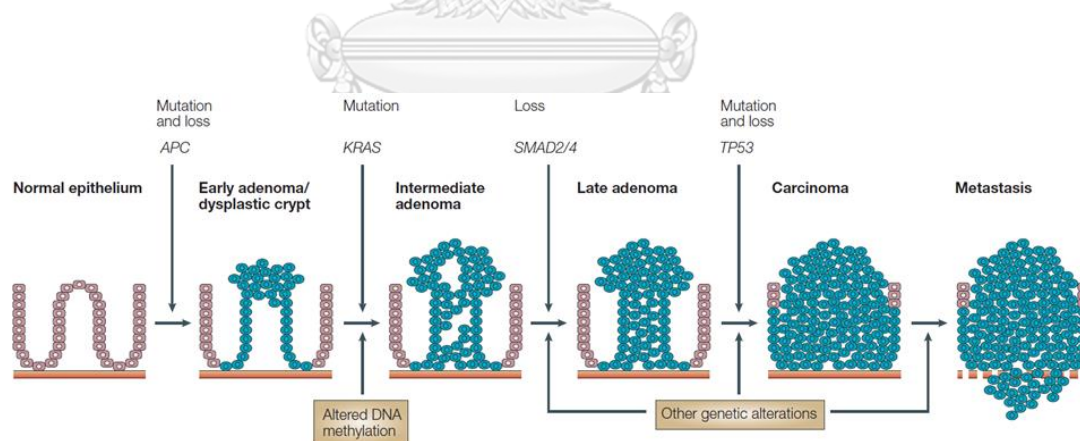


Figure 4 The colorectal adenoma-carcinoma sequence (28)

2.1.2 Symptoms of CRC

There are various clinical presentations in advanced stages of CRC. The symptoms include anemia, abdominal pain, weight loss, lower gastrointestinal tract bleeding, bowel habit change, diarrhea, constipation and bloating. Patients commonly present with several symptoms rather than one specific symptom (41).

2.1.3 Stages of CRC

According to the American Joint Committee on Cancer (AJCC) staging system, CRC can be classified into 4 stages, including 0, I, II, III and IV (42).

Stage 0: The cancer cells are still in mucosa of the colon or rectum, which is called carcinoma *in situ*.

Stage I: The cancer has grown through the mucosa and has invaded the muscular layer of the colon or rectum. It, however, has not spread to nearby tissue or lymph nodes.

Stage IIA: The cancer has grown through the wall of the colon or rectum and has not spread to nearby tissue or to the nearby lymph nodes.

Stage IIB: The cancer has grown through the layers of the muscle to the lining of the abdomen, called the visceral peritoneum. It, however, has not spread to nearby lymph nodes or anywhere else in the body.

Stage IIC: The tumor has spread through the wall of the colon or rectum and has grown into nearby structures. It, however, has not spread to nearby lymph nodes or anywhere else in the body.

Stage IIIA: The cancer has grown through the inner lining or into the muscle layers of the intestine. It has spread to 1-3 lymph nodes or to a nodule of tumor in tissues around the colon or rectum that do not appear to be lymph nodes. The cancer has not spread to other parts of the body.

Stage IIIB: The cancer has grown through the bowel wall or into surrounding organs. It has spread to 1-3 lymph nodes or to a nodule of tumor in tissues around the colon or rectum that do not appear to be lymph nodes. However, the cancer has not spread to other parts of the body.

Stage IIIC: The cancer of the colon, regardless of how deep it has grown, has spread to 4 or more lymph nodes but not spread to distant parts of the body

Stage IVA: The cancer has spread to a single distant part of the body, such as the liver or lungs.

Stage IVB: The cancer has spread to more than 1 distant part of the body.

Stage IVC: The cancer has spread to the peritoneum. It may also have spread to other sites or organs.

2.1.4 Treatment of CRC

There are multimodalities in the treatment of CRC, including surgery, radiotherapy, and chemotherapy. Surgery is the mainstay treatment of CRC. There are many techniques in cancer excision based on the anatomy of mass (43). Radiation is used in some cases of CRC. It may be used as the adjuvant therapy which can decrease the recurrent rate in some stages of CRC (44, 45). Chemotherapy is indicated in some conditions of patient including stage II or III to reduce a risk of recurrence and stage IV to control the cancer that had spread to several sites of the body (46). Many drugs are used for CRC including 5-fluorouracil (5-FU), capecitabine, oxaliplatin and irinotecan (3, 4).

5-FU is an antimetabolite which is similar in chemical structure to uracil. The mechanism of action depends on three active metabolites, including fluorouridine triphosphate (FUTP), fluoro-deoxyuridine triphosphate (FdUTP) and fluorodeoxyuridine monophosphate (FdUMP). FUTP and FdUTP get incorporated into RNA and DNA

strands, disrupting RNA and DNA synthesis, respectively whereas FdUMP inhibits thymidylate synthase (TS), a key enzyme in pyrimidine synthesis, resulting in DNA damage. In addition to 5-FU, capecitabine, an oral pro-drug of 5-FU, which is metabolized in the liver, has also been approved for treating CRC. The most common side effects of these two chemotherapeutic agents are myelosuppression, mucositis and diarrhea (47).

Oxaliplatin is the third generation of platinum based alkylating agent. Its primary mechanism of action is forming DNA adducts to prevent replication process. The main side effects of oxaliplatin are peripheral neuropathy, fatigue, neutropenia and hypokalemia (47-50).

Irinotecan is a semisynthetic derivative of the plant alkaloid camptothecin. It is converted by carboxylesterase in the liver to form an active metabolite, SN-38, which inhibits DNA topoisomerase I, making cell accumulation in the G2 or S phase. The main side effect of this drug is diarrhea (48, 51).

Due to several severe side effects associated with chemotherapeutic agents, targeted therapy has been developed to specifically attack cancer cells such as anti-vascular endothelial growth factor (anti-VEGF), anti-epidermal growth factor receptor (anti-EGFR) and multi-targeted tyrosine kinase inhibitors (TKIs). Bevacizumab, an anti-VEGF or anti-angiogenesis agent, inhibit vascular forming by binding specifically to VEGF. Anti-EGFR agents such as cetuximab and panitumumab have been approved for treating CRC patients with wild type KRAS. They are directed against the extracellular domain of EGFR, preventing ligand binding to the receptors. In addition to monoclonal antibodies, regorafenib, a multi-targeted tyrosine kinase inhibitor (TKI), has recently been approved for CRC. The drug binds to adenosine triphosphate (ATP) binding site of the tyrosine kinase domain of the several receptors such as VEGFR, platelet-derived

growth factor receptor, and KIT (stem cell factor receptor), resulting in inhibition of cell growth (4).

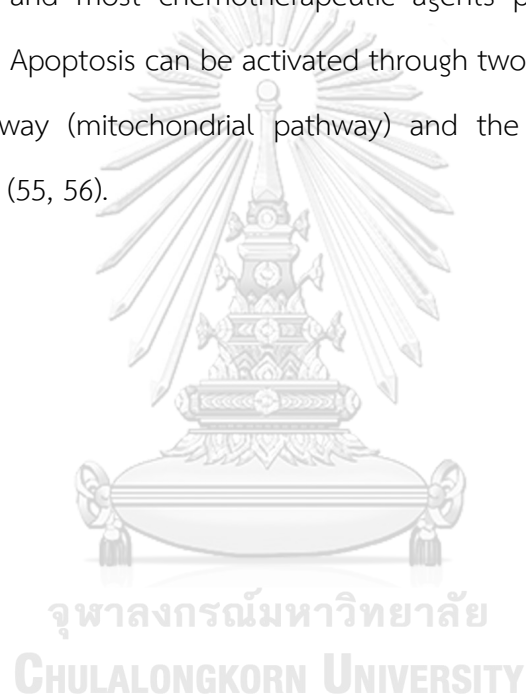
2.2 Reactive Oxygen Species

Reactive oxygen species (ROS), such as superoxide anion (O_2^-), hydrogen peroxide (H_2O_2) and hydroxyl radicals ($OH\bullet$), are natural byproducts of aerobic metabolism. ROS is associated with an oxidative stress, which occurs as a result of an imbalance between free radical production and elimination. Oxidative stress can cause disruption of mitochondrial membrane integrity and subsequently release of cytochrome C, which in turn activates intrinsic apoptotic machinery, leading to the cell death. ROS play important roles in cell signaling, homeostasis, cell cycle arrest, cellular senescence, and apoptosis (5-10).

Generally, low concentration of ROS can assist cell proliferation and survival, however high concentration of ROS is cytotoxic. Excessive production of ROS in cancer cells can induce apoptosis through oxidative stress. Many chemotherapeutic agents such as doxorubicin, vinblastine, camptothecin and cisplatin exhibit antitumor activity partly through increased ROS, leading to DNA damage (14, 15). In addition to currently marketed anticancer drugs, the effect of natural compounds on ROS generation in cancer have been extensively investigated. Previous study demonstrated that curcumin-induced apoptosis via ROS production, resulting in activation of caspase-3, modulation of pre-mRNA processing factor 4B (Prp4B) and expression of p53 in HCT-15 colon cancer cells (52). Similarly, dehydrozingerone, a structural analogue of curcumin, induced cell cycle arrest at G2/M phase and apoptosis through the accumulation of ROS in HT-29 human colon cancer cells (53). Moreover, it was reported that the active ingredients of grape seed extract such as epigallocatechins, anthocyanins and gallic acid generated ROS and increased Ca^{2+} level, concomitantly with ERK inactivation, eventually leading to apoptosis in Caco-2 colon cancer cells (54).

2.3 Apoptosis

Apoptosis is the programmed cell death which is the normal process of the cell to conserve homeostasis in higher organism. Cell signaling and caspases are central mediators of apoptosis events. Characteristics of apoptosis include cell shrinkage, nuclear fragmentation, chromatin condensation and cell membrane blebbing (55, 56). Since apoptosis is critically important for cell survival, deregulation of apoptosis is involved in development and progression of cancer. Cancer cells can modulate and disturb apoptosis and most chemotherapeutic agents promote cells to undergo apoptosis (18, 19). Apoptosis can be activated through two major pathways, including the intrinsic pathway (mitochondrial pathway) and the extrinsic pathway (death receptor pathway) (55, 56).



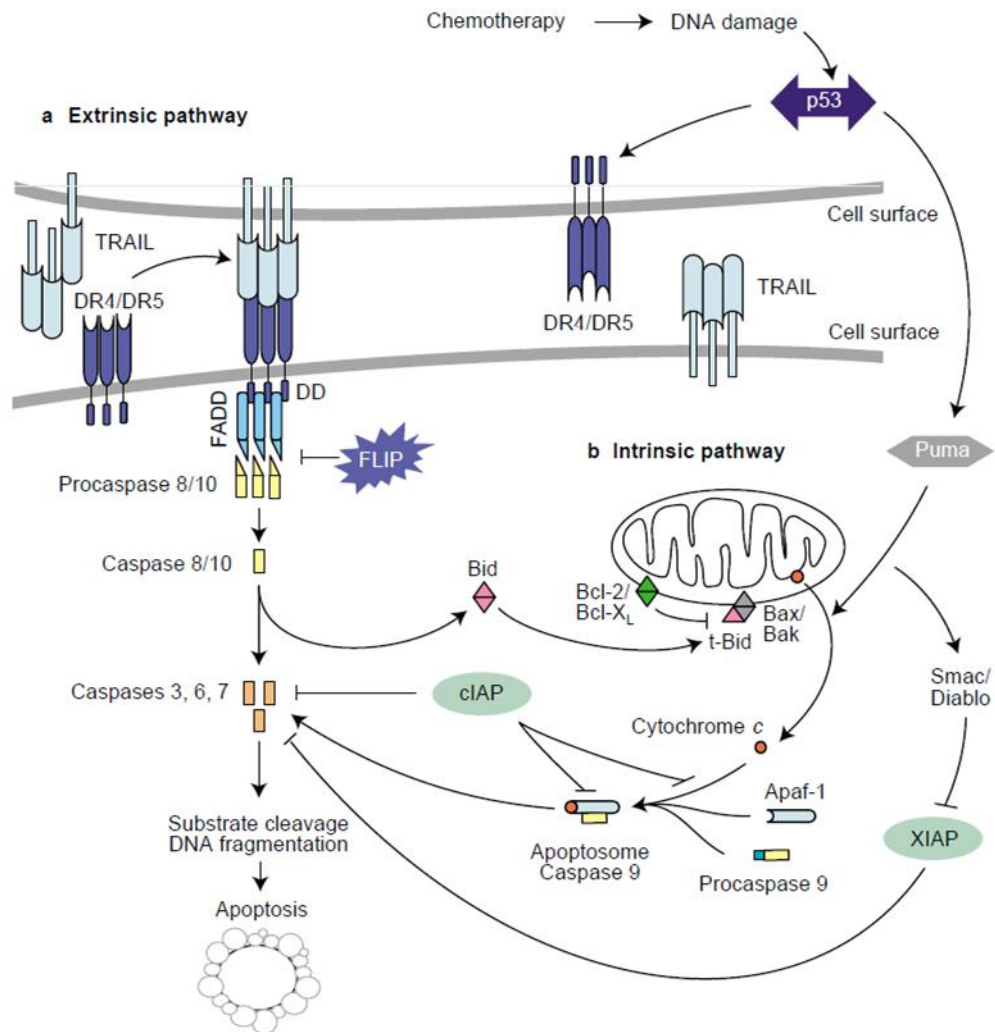


Figure 5 Intrinsic and extrinsic apoptosis pathways (57)

2.3.1 Death-receptor-induced extrinsic apoptotic pathway

The specific ligands activate the death receptors including, tumor necrosis factor receptor (TNFR), Fas receptor (FasR), death receptor 3 (DR3), TNF-related apoptosis-inducing ligand receptors1 (TRAILR1 or DR4), TRAILR2 (or DR5) and DR6, forming death-inducing signaling complex (DISC) by incorporating with adaptor protein and procaspases (procaspase 8 or 10). Procaspase 8 or 10 are then cleaved, becoming active caspase 8 or 10, which further activates the downstream effector caspases, including caspase-3, 6, or 7 to induce apoptosis (57, 58).

2.3.2 Mitochondrial-apoptosome-mediated intrinsic apoptotic pathway

DNA damage stimuli such as free radical, ultraviolet irradiation (UV), and chemotherapeutic agents can induce internal cellular stresses by activating BH3 only pro-apoptotic Bcl-2 proteins such as PUMA and NOXA, which are inhibitors of anti-apoptotic Bcl-2 proteins such as Bcl-2 and Bcl-xl. Normally, anti-apoptotic Bcl-2 proteins inhibit pro-apoptotic Bcl-2 effector proteins such as Bax and Bak which is normally stabilize mitochondria outer membrane permeabilization (MOMP) (29). Apoptotic stimuli induce oligomerization of pro-apoptotic Bcl-2 effector proteins, forming pores, resulting in release of apoptogenic factors, including apoptosis-inducing factor (AIF), endonuclease G (Endo G), second mitochondria-derived activator of caspases/direct IAP binding protein with a low iso-electric point (Smac/DIABLO) and cytochrome C from intermembrane space. AIF and Endo G induce chromatin condensation and DNA fragmentation in nucleus whereas Smac/DIABLO inhibits X-linked inhibitor of apoptosis protein (XIAP). Cytochrome C binds with the apoptosis protein-activating factor 1 (Apaf-1) and procaspase-9 to form the protein complex known as “apoptosome”, resulting in autocatalytically cleavage of procaspase-9. Active caspase-9 then cleaves and activates effector caspases, inducing apoptosis. (30-32)

The intrinsic apoptotic pathway is regulated by members of the Bcl-2 family proteins. The Bcl-2 family proteins are divided into three groups depending on Bcl-2 homology (BH) domain organization (Figure 6) (59-61).

- (i) Anti-apoptotic Bcl-2 proteins, such as Bcl-2 and Bcl-xl, consist of BH1, BH2, BH3 and BH4 domains. These proteins prevent apoptosis by inhibiting the function of the pro-apoptotic effector proteins.

- (ii) Pro-apoptotic Bcl-2 effector proteins, such as Bak and Bax, consist of BH1, BH2 and BH3 domain. The function of these proteins is promoting apoptosis through the mitochondria outer membrane permeabilization (MOMP).
- (iii) BH3 only pro-apoptotic Bcl-2 proteins, such as Noxa and Puma, consist of BH3 domain. The function of these proteins induces apoptosis by inhibiting anti-apoptotic Bcl-2 proteins or activating pro-apoptotic Bcl-2 effector proteins.

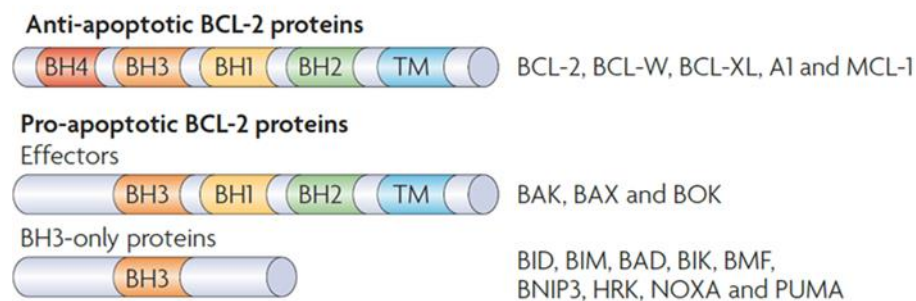


Figure 6 Bcl-2 family proteins (56)

2.4 MAPK Signaling pathway

The mitogen-activated protein kinase (MAPK) signaling pathway regulates wide range of cellular activities and physiological processes such as cell growth, differentiation, motility, metabolism, survival and apoptosis as well as embryogenesis (62). There are three major subfamilies of MAPK pathway, including the extracellular signal-regulated kinases (ERK), the c-Jun N-terminal kinase (JNK) and the p38 MAPK. ERK1/2 is the one of most important subfamilies of MAPK signaling pathway. Several studies demonstrated that activation of ERK1/2 MAPK signaling pathway is involved in tumorigenesis and progression of CRC (63). The ERK1/2 MAPK signaling is commonly activated through the mutation of RAS and RAF. In CRC, the mutation of KRAS gene is approximately 35-45% whereas the mutation of NRAS and BRAF occur approximately 4% and 8%, respectively (64). The mechanism of ERK1/2 cascade is initiated by a

variety of extracellular signals, including growth factors, which bind to a receptor tyrosine kinase. Binding of ligand to its specific receptors recruit adaptor proteins such as Grb2 and guanine nucleotide exchange factor (GEF) such as Son of sevenless (Sos) to receptor which in turn activates Ras by switching from inactive GDP-bound form to the active GTP-bound form. Activated Ras phosphorylates Raf protein and subsequently activated Raf protein phosphorylates MEK1/2 which further activates ERK1/2 by phosphorylation (63-67). Activated ERK1/2 can promote cell survival and inhibit apoptosis by downregulating the activity of pro-apoptotic molecules or upregulating the activity of anti-apoptotic molecules via activation of their transcription (Figure 7). It is commonly known that DNA damage stimuli such as etoposide, adriamycin, platinum compounds, ionizing irradiation and UV can induce apoptosis through activation of ERK1/2 (62).

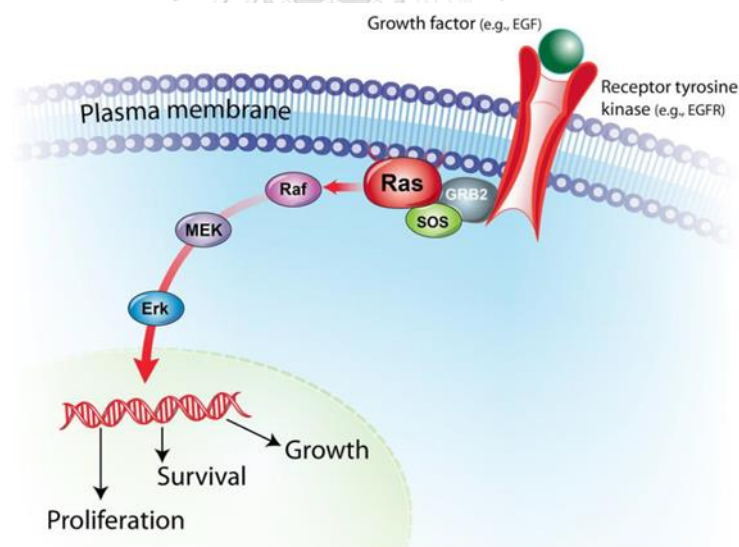


Figure 7 ERK1/2 MAPK signaling pathway (68)

2.5 PI3K/AKT signaling pathway

Phosphatidylinositol 3-kinase (PI3K)/AKT signaling pathway is involved in cell growth, proliferation, metabolism, motility, survival and apoptosis (69). Binding of EGF molecules to their receptors activates PI3K, which in turn phosphorylates

phosphatidylinositol 4,5-bisphosphate (PIP₂) to phosphatidylinositol-3,4,5-trisphosphate (PIP₃). PIP₃ functions as a docking site to recruit phosphoinositide-dependent kinase 1 (PDK1) and AKT to bind to PIP₃ via pleckstrin (PH) domains. Then, AKT is activated by phosphorylation of PDK1 and the mammalian target of rapamycin (mTOR), leading to dissociation of AKT to the cytosol. Activated AKT regulates a wide range of proteins by phosphorylation, resulting in cell growth, survival and proliferation (Figure 8). It was shown that PI3K/AKT signaling pathway is frequently activated in CRC (70).

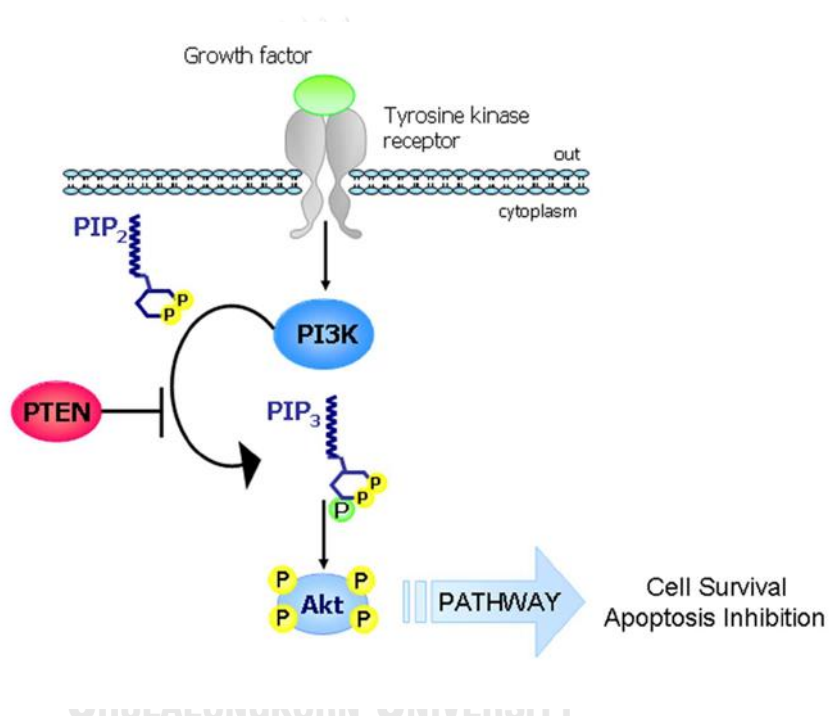


Figure 8 PI3K/AKT signaling pathway (71)

2.6 Mansonone G and its derivatives

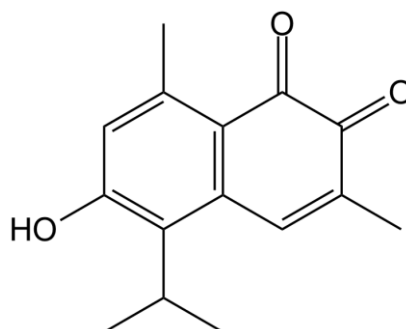


Figure 9 Structure of mansonone G (MW 244.29 g/mol) (72, 73)

Mansonone is a 1,2-naphthoquinone, isolated from *Mansonia gagei* Drumm (21, 73) (Figure 9). *Mansonia gagei* Drumm is a Thai traditional medicine plant that belongs to the Sterculiaceae family. It is also known as sandalwood and locally called Chan-cha-mod, Chan, Chan-hom, Chan-pa-ma and Chan-khao in Thailand (74-76). *Mansonia gagei* Drumm is a deciduous plant and the height ranges around 10-20 meters. The color of its smooth surfaced bark is whitish grey and the heartwood is dark brown. It has round leaf; white flower and their fruit is spindle shaped (77). Thai sandalwood regimen is established in the National List of Essential Medicine (NLEM) 2012. The heartwood of *Mansonia gagei* Drumm is locally used as an antidepressant, antiemetic, cardiac stimulant and refreshment agent (20, 74). Previous studies have reported the chemical constituents from the heartwoods of *Mansonia gagei* Drumm are mansonones (C, E, F, G, H, I, N, O, P and S) and coumarins (mansorin A, B, C) (21, 73, 75, 78).

Pharmacological effects of mansonones

Antibacterial effect

In 2008, Boonsri et al. found that mansonone E, isolated from the heartwood of *Thespesia populnea*, exhibited antibacterial activity against *Bacillus subtilis* with the minimum inhibitory concentration (MIC) of 4.69 µg/ml (24). Moreover, it was shown that mansonone E had high antibacterial activity against both *Xanthomonas oryzae*

pv. *Oryzae* (Xoo) and *Xanthomonas oryzae* pv. *Oryzicola* (Xoc). The MIC and minimum bactericidal concentration (MBC) were 7.8 and >500 µg/ml, respectively (79).

Anti-fungal effect

A previous study demonstrated that mansonone E, extracted from *Mansonia gagei* Drumm, displayed the antifungal activity against *Phytophthora parasitica* with 94% inhibition at 1,000 µg/ml. Mansonone C, mansonone B and mansonone G also showed potent activities against this fungus with 84, 81, and 61% inhibition, respectively (79). Tiew et al. found that mansonone C and E had antifungal activity against *Candida albicans* with a minimal amount to inhibit fungal growth on a silica gel TLC plate of 0.15 µg and 2.5 µg, respectively (75). They also exhibited antifungal activity against *Cladosporium cucumerinum* with a minimal inhibitory amount of 0.6 µg and 0.6 µg, respectively (75).

Anti-estrogenic effect

El-Halawany et al. reported that mansonone G and its derivative displayed a potent anti-estrogenic activity by competing with estrogen for binding to estrogen receptor (ER). Moreover, acetyl mansonone G showed a 10-fold increase in its binding ability to ER when compared to mansonone G with an IC_{50} of acetyl mansonone G was 630 µM (22).

Anti-oxidant effect

A previous study indicated that mansonone N, isolated from *Mansonia gagei* Drumm, had the radical scavenging activity towards the 2,2-diphenyl-1-hydrazyl (75). Similarly, using a thiobarbituric acid method, Kim et al demonstrated that mansonone E and F, isolated from the root bark of *Ulmus davidiana*, exhibited antioxidant properties. Mansonone E and F inhibited microsomal lipid peroxidation with IC_{50} values of 0.03 and 0.04 µg/ml, respectively (80).

Anti-adipogenic effect

Recently, mansonone G was found to inhibit differentiation of 3T3-L1 adipocyte cells, with a 40% decrease in lipid accumulation at 10 μM via suppression of peroxisome proliferator-activated receptor- γ -mediated adipogenic gene expression (72).

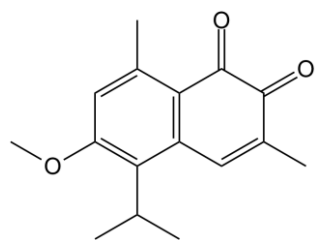
Anti-cancer effect

A previous study reported that mansonone E and F, isolated from *Ulmus pumila*, exhibited anticancer effect in many types of cancer. The IC_{50} values of mansonone E were 2.2, 7.9, 3.1 and 0.9 μM and IC_{50} values of mansonone F were 13.3, 30.5, 29.4 and 3.0 μM in melanoma (A375-S2), cervical cancer (HeLa), breast cancer (MCF-7) and lymphoma (U937), respectively. Mansonone E could induce apoptosis on HeLa cells by breaking oligonucleosome, activating caspase-3, decreasing the expression of anti-apoptotic proteins, Bcl-2 and Bcl-xl, and increasing the expression of a pro-apoptotic protein, Bax (23). Similarly, Sompong et al demonstrated that mansonone E, extracted from *Thespesia populnea*, displayed anticancer effect in several types of cancer including breast cancer (MCF-7), cervical cancer (HeLa), colorectal cancer (HT-29) and oral cavity cancer (KB) and its IC_{50} were 0.05, 0.55, 0.18 and 0.4 μM , respectively (24). Furthermore, cytotoxicity of mansonone E, extracted from the root bark of *Ulmus davidiana*, has been found against various human leukemia cell lines, including HL60, K562, THP-1 and U937 (25).

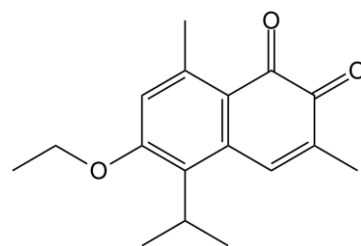
In 2003, Tiew et al. extracted several mansonones including mansonone C, E, N, O, P, H, G from the heartwood of *Mansonia gagei* Drumm and found that mansonone G (MG) is a major compound of the extract. The extraction yield was approximately 5 g (75). Hairani et al. has reported that mansonones including mansonone C, E, G and H were isolated from the heartwood of *Mansonia gagei* Drumm.

Since MG displayed a good anti-bacterial activity, its ether analogues were then synthesized. Later, it was found that increasing alkyl chain length of ether analogues of MG results in higher antibacterial activity than the parent MG (20). Moreover, a recent study demonstrated that ten ether analogues of MG (G01-G10) (Figure10) suppressed adipocyte differentiation more potently than the parent compound (72).

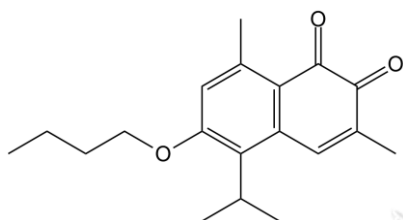




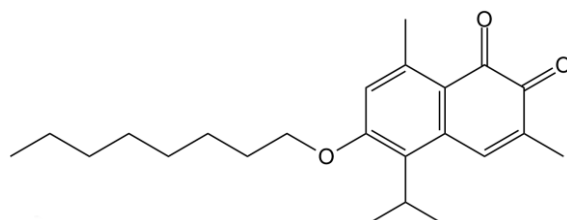
G01 (MW 258 g/mol)



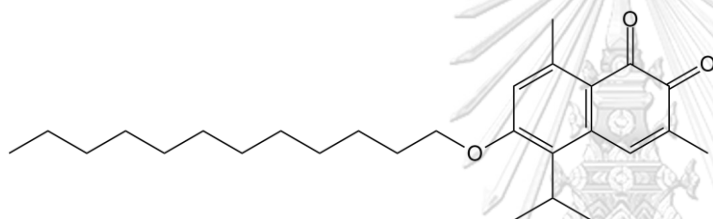
G02 (MW 272 g/mol)



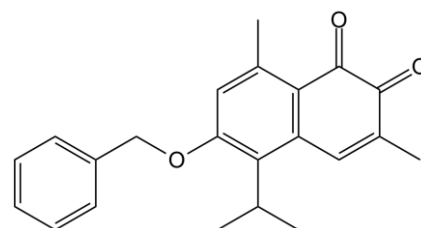
G03 (MW 300 g/mol)



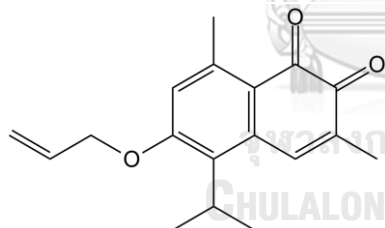
G04 (MW 356 g/mol)



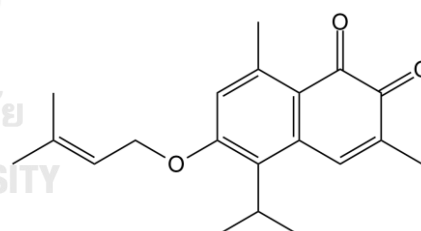
G05 (MW 412 g/mol)



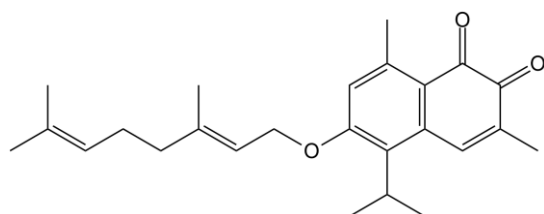
G06 (MW 334 g/mol)



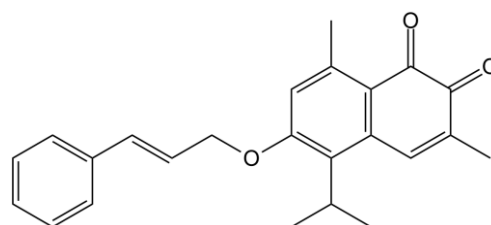
G07 (MW 284 g/mol)



G08 (MW 312 g/mol)



G09 (MW 380 g/mol)



G10 (MW 360 g/mol)

Figure 10 Structures of mansonone G derivatives

CHAPTER III

MATERIALS AND METHODS

3.1 Equipment

- Analytical balance (Mettler Toledo, Switzerland)
- Autopipette (Brand, Germany)
- Autoclave (Sanyo, Japan)
- Biohazard laminar flow hood (Labconco, USA)
- Controller pipette (Gilson, USA)
- CO₂ incubator (Thermo, USA)
- Centrifuge (Hettich, Germany)
- Fluorescence flow cytometer (BD Bioscience, USA)
- Gel electrophoresis (Hoefer, USA)
- Light microscope (Nikon, Japan)
- Microplate reader (Thermo, Finland)
- pH meter (Mettler Toledo, Switzerland)
- TE 22 mini tank transfer unit (Hoefer, USA)
- Temperature control centrifuge (Eppendorf, Germany)
- Vortex mixer (Scientific Industries, USA)
- Water bath (IKA Labortechnik, Germany)

3.2 Materials

- 15 ml conical tube (Corning Inc., USA)
- 6-well plate (Corning Inc., USA)
- 96-well plate (Corning Inc., USA)

- 25 cm² rectangular cell culture flask (Corning Inc., USA)
- Polyvinylidene difluoride (PVDF) membrane (Merck, Germany)

3.3 Reagents

- Ammonium persulfate (Sigma, USA)
- Annexin V, Fluorescein conjugate (FITC) (Life technologies, USA)
- Bromophenol blue (Sigma, USA)
- β -mercaptoethanol (Sigma, USA)
- Bio-Rad Protein assay kit (Bio-Rad, USA)
- Dimethyl sulfoxide (DMSO) analytical grade (Sigma, USA)
- Dimethyl sulfoxide (DMSO) molecular grade (Sigma, USA)
- Dichloro-dihydro-fluorescein diacetate (DCFH-DA) (Sigma, USA)
- Dulbecco's Modified Eagle Medium (DMEM) (Gibco, USA)
- Fetal bovine serum (Gibco, USA)
- *N*-acetyl cysteine (NAC) (Sigma, USA)
- Penicillin-streptomycin (Gibco, USA)
- Primary antibodies (Cell Signaling, USA)
 - Bak Rabbit monoclonal antibody (25 kDa)
 - Bax Rabbit monoclonal antibody (20 kDa)
 - Bcl-2 Rabbit monoclonal antibody (26 kDa)
 - Bcl-xl Rabbit monoclonal antibody (30 kDa)
 - GAPDH Rabbit monoclonal antibody (37 kDa)
 - PARP Rabbit monoclonal antibody (116, 89 kDa)

- Phospho-p44/42 MAPK (ERK1/2) Rabbit monoclonal antibody (44, 42 kDa)
- p44/42 MAPK (ERK1/2) Rabbit monoclonal antibody (44, 42 kDa)
- Phospho-Akt Rabbit monoclonal antibody (60 kDa)
- Akt (pan) Rabbit monoclonal antibody (60 kDa)
- Propidium iodide (Santa Cruz Biotechnology, USA)
- Protease inhibitors (Sigma, USA)
- Protogel (National Diagnostic, USA)
- Pyronin Y (Sigma, USA)
- RIPA lysis buffer (Thermo, USA)
- Roswell Park Memorial Institute (RPMI)-1640 medium (Gibco, USA)
- Secondary antibody (Cell Signaling, USA)
 - Anti-IgG, horseradish peroxidase (HRP)-linked antibody
- Sodium dodecyl sulfate polyacrylamide (SDS) (EM science, USA)
- Tetramethylethylenedimine (TEMED) (EM science, USA)
- Tris base (EM science, USA)
- Tween 20 (Sigma, USA)
- 3-(4, 5-dimethylthiazol-2-yl)-2,5-diphenyltetrazolium bromide (MTT) (Sigma, USA)
- 0.4% trypan blue dye (Sigma, USA)
- 0.25% trypsin-EDTA (Gibco, USA)

3.4 Methods

3.4.1 Cell culture

The human colon carcinoma cell lines, HCT-116 and HT-29, were obtained from the American Type Culture Collection (ATCC). HCT-116 cells were maintained in Roswell Park Memorial Institute (RPMI) 1640 medium supplemented with 10% fetal bovine serum (FBS), 100 U/mL penicillin and 100 µg/mL streptomycin. HT-29 cells were cultured in Dulbecco's modified Eagle's medium (DMEM) containing 10% FBS, 100 U/mL penicillin and 100 µg/mL streptomycin. Cells were grown in a humidified 5% CO₂ incubator at 37°C.

The human normal cell lines including primary dermal fibroblasts, PCS201-010 and normal colon cells, CRL-1790, were obtained from the American Type Culture Collection (ATCC). Both cells were maintained in Dulbecco's modified Eagle's medium (DMEM) containing 10% FBS, 100 U/mL penicillin, 100 µg/mL streptomycin and 4.5 g/L glucose. Cells were grown in a humidified 5% CO₂ incubator at 37°C.

3.4.2 Preparation of mansonone G and its derivatives stock solution

Mansonone G (MG) and its derivatives including G01, G02, G03, G04, G05, G06, G07, G08, G09 and G10 were kindly provided by Asst. Prof. Warinthorn Chavasiri, Department of Chemistry, Faculty of Science, Chulalongkorn University. A 50 mM stock solutions of MG and its ten derivatives were prepared in dimethyl sulfoxide (DMSO). In the experiments, the stock solution was diluted in culture medium to give appropriate final concentrations and the final concentration of DMSO was constantly kept at 0.2%. The 0.2% DMSO was used as a vehicle control.

3.4.3 Determination of cell viability by MTT assay

Viable cells with active metabolism can convert 3-(4, 5-dimethylthiazol-2-yl)-2,5-diphenyltetrazolium bromide (MTT) into a purple colored formazan product by

mitochondrial succinate dehydrogenase enzyme. The absorbance of a color solution can be measured spectrophotometrically at 570 nm.

The cytotoxic effects of MG and its derivatives including G01, G02, G03, G04, G05, G06, G07, G08, G09 and G10 were determined by MTT assay. Briefly, HCT-116, HT-29, PCS201-010 or CRL-1790 cells were seeded into 96-well plates at a density of 5×10^4 cells/ml and incubated overnight at 37 °C. HCT-116 and HT-29 cells were then treated with MG or its derivatives, including G01, G02, G03, G04, G05, G06, G07, G08, G09 and G10, at the concentrations of 0.1, 1, 10 and 100 μ M. PCS201-010 cells were treated with G03, G04, G07 and G10 at the concentrations of 1, 10 and 100 μ M while CRL-1790 cells were treated with G07 at the concentrations of 1.25, 5, 10 and 20 μ M, or 0.2% DMSO in complete medium for 48 h. Next, 15 μ L of MTT (0.5 mg/mL) was added into each well and incubated for 4 h. After removing supernatant, 150 μ L of DMSO was added to solubilize formazan crystals. Finally, the optical density was measured at 570 nm using a microplate reader (Thermo, Finland).

3.4.4 Analysis of apoptosis using Annexin V-FITC/PI staining

In the early stages of apoptosis, cells translocate phosphatidylserine (PS) from the inner plasma membrane to the cell surface, which can be detected by annexin V-fluorescein isothiocyanate (FITC) conjugate. During late apoptosis and necrosis, the integrity of the plasma membrane is lost, allowing propidium iodide (PI) to pass through the membrane. Therefore, annexin V-FITC/PI staining can be used to determine whether cells are alive or undergo apoptosis or necrosis based on differences in plasma membrane integrity and permeability.

HCT-116 and HT-29 cells were seeded into 6-well plates at a density of 5×10^4 cells/ml and incubated overnight. HCT-116 cells were then treated with G07 at concentrations of 2.5, 5 and 10 μ M for 24 h. HT-29 cells were treated with G07 at concentrations of 5, 10 and 20 μ M for 24 h. After that, the cells were collected by

trypsinization and centrifugation at 1,500 rpm for 5 min. The cell pellets were washed twice with cold PBS. After re-suspending cells with 400 μ l of assay buffer, the cells were stained with 3 μ l of Annexin V-FITC (Invitrogen, USA) and 1 μ l of PI (Santa Cruz Biotechnology, USA) for 15 min in the dark. The stained cells were analyzed using flow cytometer (BD LSR II, Biosciences).

3.4.5 Evaluation of protein expression using western blot analysis

Effects of G07 on expression of apoptotic-related proteins, including Bak and Bax (pro-apoptotic proteins), Bcl-2 and Bcl-xl (anti-apoptotic proteins), and PARP and signaling pathway proteins, including, ERK1/2, phospho-ERK1/2, Akt and phospho-Akt were evaluated by western blotting. GAPDH was used as an internal control.

HCT-116 cells were treated with G07 at concentrations of 2.5, 5 and 10 μ M whereas HT-29 cells were treated with G07 at concentrations of 5, 10 and 20 μ M for 24 h. Treated cells were lysed with RIPA buffer (Thermo scientific, USA). Protein concentration of cell lysate was determined using the Bio-Rad DC Protein assay reagents (Bio-Rad, USA). Twenty micrograms of protein lysate from cells were separated on an 8% sodium dodecyl sulfate polyacrylamide gel electrophoresis (SDS-PAGE) and then transferred to a PVDF membrane. The membrane was incubated with 3% non-fat dry milk (NFDM) for 1 h for preventing non-specific binding. The membrane was then incubated with Bak (dilution 1:1000), Bax (dilution 1:1000), Bcl-2 (dilution 1:1000), Bcl-xl (dilution 1:1000), PARP (dilution 1:1000), phospho-p44/42 MAPK (ERK1/2) (dilution 1:1000), p44/42 MAPK (ERK1/2) (dilution 1:1000), phospho-Akt (dilution 1:1000), Akt (pan) (dilution 1:1000) or GAPDH (dilution 1:1000) (Cell Signaling, USA) primary antibody overnight at 4 °C. The membrane was then incubated with horseradish peroxidase (HRP)-conjugated secondary antibody (dilution 1:2000) (Cell signaling, USA) for 2 h at room temperature. Protein bands were detected using chemiluminescence detection

system (Pierce, USA) and analyzed using Image Studio software (LI-COR, Lincoln, NE, USA).

3.4.6 Determination of intracellular ROS using DCFH-DA assay

Dichloro-dihydro-fluorescein diacetate (DCFH-DA) is a fluorogenic dye that measures ROS within the cell. After diffusion into the cell, DCFH-DA is deacetylated by cellular esterase to a non-fluorescent compound, which is later oxidized by ROS into 2',7'-dichlorofluorescein (DCF). A highly fluorescent DCF can be quantified by fluorescence spectroscopy.

HCT-116 and HT-29 cells were seeded into 96-well plates at a density of 5×10^4 cells/ml and incubated overnight. Both cells were incubated with 100 μ l of 10 μ M DCFH-DA in Hank's buffered salt solution (HBSS) at 37 °C in the dark for 30 min. Subsequently, the cells were washed with PBS. HCT-116 cells were then treated with G07 at concentrations of 2.5, 5 and 10 μ M whereas HT-29 cells were treated with G07 at concentrations of 5, 10 and 20 μ M for 24 h. After that, the cells were washed twice with PBS and 200 μ l of 1% triton-X in 0.3 NaOH was added. The fluorescence intensity was measured at an excitation wavelength of 485 nm and an emission wavelength of 535 nm using a fluorescence microplate reader (Thermo, Finland).

3.4.7 Statistical analysis

All data are reported as mean \pm standard error of mean (SEM) from three independent experiments performed in triplicate. Statistical analysis was performed by one-way analysis of variance (ANOVA) followed by LSD and student's t-test was used to compare significant difference between two groups using SPSS software program. Difference is considered significant if p value < 0.05.

CHAPTER IV

RESULTS

4.1 Effect of mansonone G and mansonone G derivatives on the viability of colorectal cancer cells

Initially, the effects of mansonone G (MG) and its derivatives on the viability of two CRC cell lines, p53 wild-type HCT-116 and p53 mutant HT-29, were investigated. Cells were incubated with MG and its derivatives at the concentrations of 0.1, 1, 10 and 100 μ M for 48 h. Cell viability was assessed using the MTT assay. As shown in Figure 11 and Figure 12, MG and its derivatives significantly inhibited the growth of the two tested human CRC cell lines in a concentration-dependent manner ($P < 0.001$). The values of the half maximal inhibitory concentration (IC_{50}) of MG and its derivatives were illustrated in Table 1. Notably, tested MG derivatives, including G01, G02, G03, G04, G05, G06, G07, G08, G09 and G10 were more cytotoxic to cancer cells than the parent compound. Of all MG derivatives, G04 exhibited the most potent cytotoxicity toward HCT-116 cells, followed by G10, G06 and G07, respectively (Table 1). Similarly, G04, G07, G08 and G03 displayed potent cytotoxicity against HT-29 cells (Table 1). Taken together, G04 followed by G07, G03 and G10 were very toxic to both CRC cell lines.

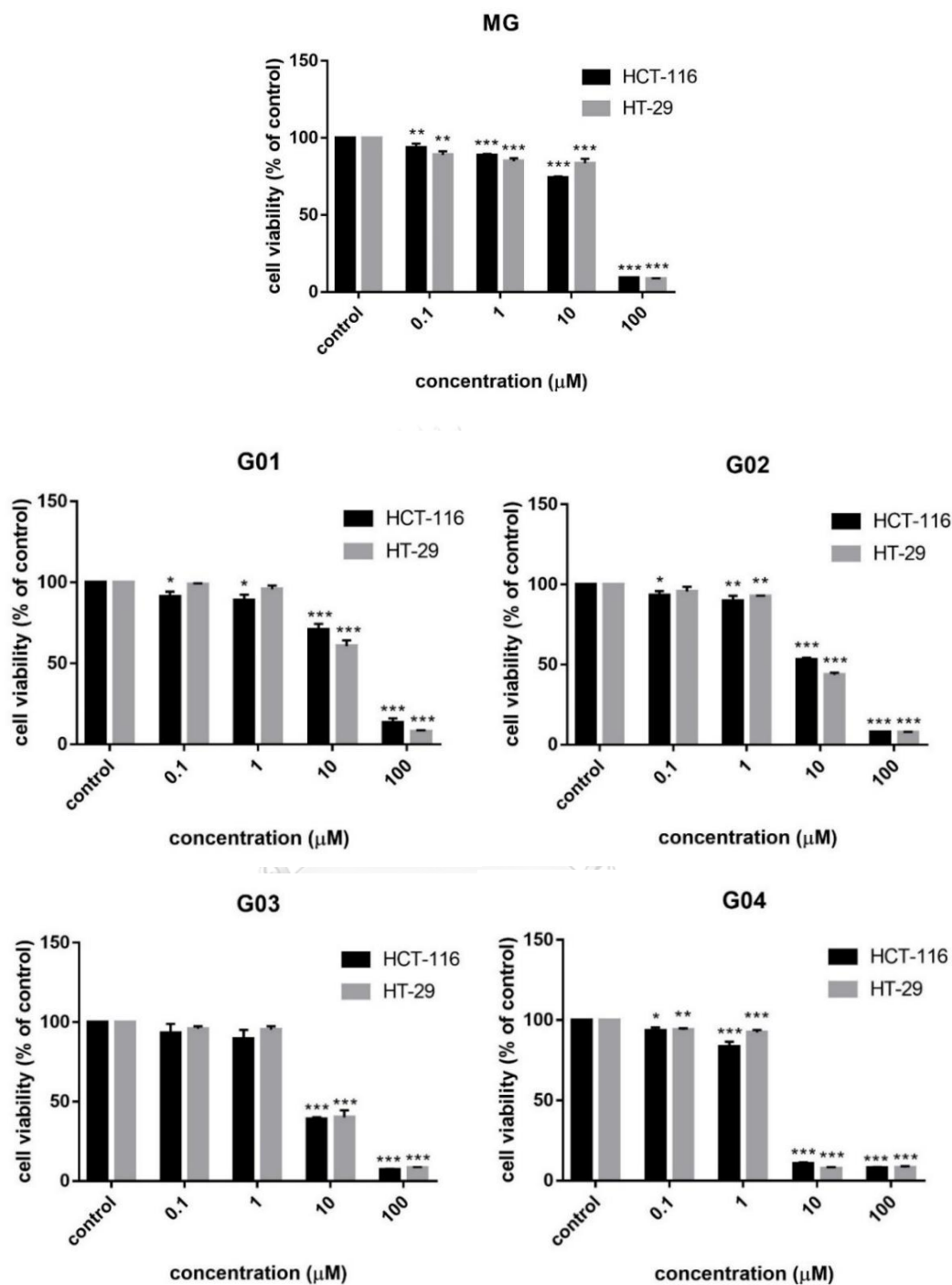


Figure 11 Effects of MG and its derivatives (G01-G04) on the viability of HCT-116 and HT-29 cells. Both cell lines were treated with MG or its derivatives at 0.1, 1, 10 and 100 μM for 48 h. Cell viability was evaluated using MTT assay. Each value is expressed as the mean \pm SEM (n=3). * $P < 0.05$, ** $P < 0.01$, *** $P < 0.001$ compared with vehicle control (0.2% DMSO).

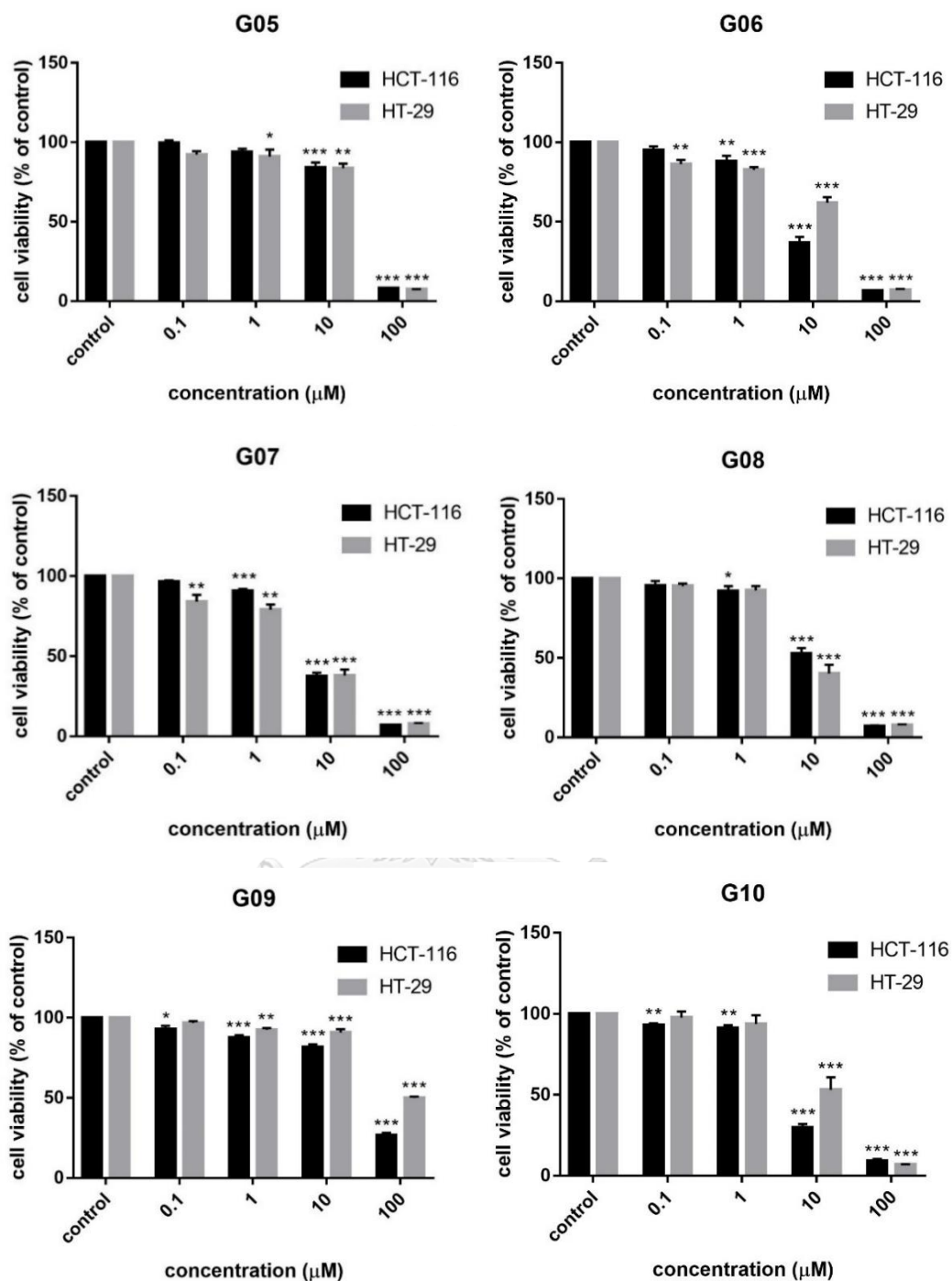


Figure 12 Effects of mansonone G derivatives (G05-G10) on the viability of HCT-116 and HT-29 cells. Both cell lines were treated with MG or its derivatives at 0.1, 1, 10 and 100 μM for 48 h. Cell viability was evaluated using MTT assay. Each value is expressed as the mean ± SEM (n=3). *P<0.05, **P<0.01, ***P<0.001 compared with vehicle control (0.2% DMSO).

Table 1: IC₅₀ values of MG and its derivatives on HCT-116 and HT-29 cells

Compounds	IC ₅₀ (μM)	
	HCT-116	HT-29
MG	20.74 ± 0.51	25.55 ± 2.08
G01	20.86 ± 3.10	15.07 ± 1.91
G02	10.60 ± 0.65	8.43 ± 0.81
G03	6.63 ± 0.60	8.09 ± 1.13
G04	2.77 ± 0.20	3.24 ± 0.21
G05	26.59 ± 2.39	26.68 ± 2.08
G06	6.13 ± 0.59	13.62 ± 1.42
G07	6.54 ± 0.47	5.66 ± 1.13
G08	10.83 ± 1.44	7.53 ± 1.20
G09	37.85 ± 1.42	98.59 ± 3.37
G10	5.16 ± 0.53	9.89 ± 1.49

4.2 Effects of mansonone G derivatives on the viability of normal cells

Next, toxicity of G03, G04, G07 and G10 was determined on normal fibroblast cells, PCS201-010. Cells were treated with the four MG derivatives at 1, 10 and 100 μM for 48 h. Although G04 and G07 were highly effective in controlling the growth of CRC cells, the results showed that G04 was more toxic to normal fibroblast cells than G07 (Figure 13). To confirm whether G07 was not too toxic to normal cells, toxicity of G07 was also evaluated on normal colon cells, CRL-1790. As shown in Figure 14, G07 significantly decreased the viability of CRL-1790 cells in a concentration-dependent manner ($P < 0.001$). The IC₅₀ value was 22.07 ± 1.10 μM. Given that G07 was more toxic to CRC cells than normal colon cells, anticancer activity and the underlying mechanisms of G07 were further studied.

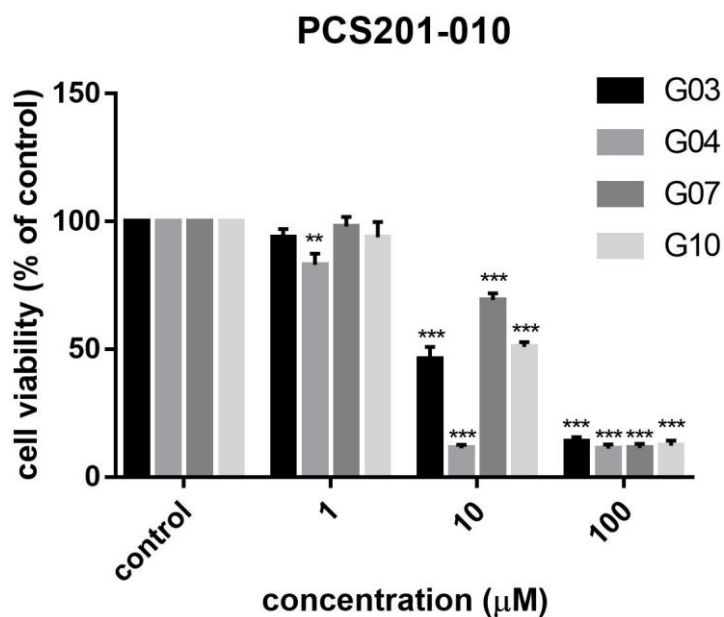


Figure 13 Effects of G03, G04, G07 and G10 on the viability of PCS201-010 cells. Cells were treated with G03, G04, G07 and G10 at 1, 10 and 100 μM for 48 h. Cell viability was evaluated using MTT assay. Each value is expressed as the mean \pm SEM (n=3). **P<0.01, ***P<0.001 compared with vehicle control (0.2% DMSO).

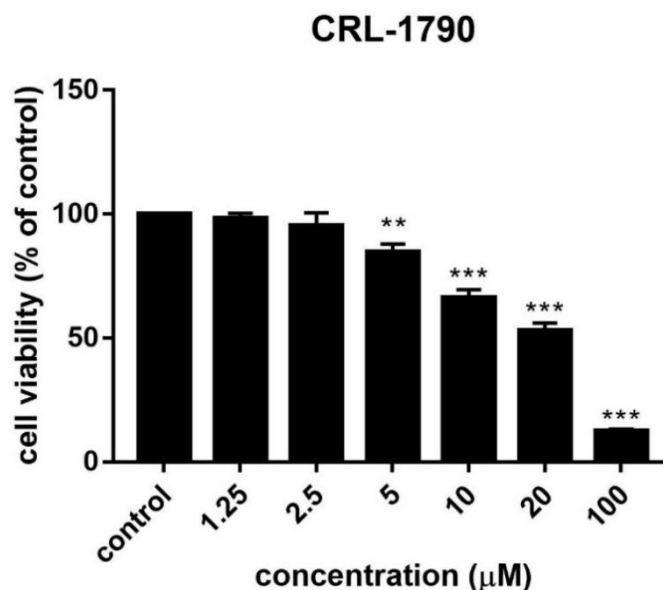


Figure 14 Effects of G07 on the viability of CRL-1790 cells. Cells were treated with G07 at 1.25, 2.5, 5, 10, 20 and 100 µM for 48 h. Cell viability was evaluated using MTT assay. Each value is expressed as the mean \pm SEM (n=3). **P<0.01, ***P<0.001 compared with vehicle control (0.2% DMSO).

4.3 Effect of G07 on the viability of HCT-116 cells

As illustrated in Figure 15, HCT-116 cells significantly inhibited the growth of p53 wild-type HCT-116 cells in a concentration-dependent manner (P<0.01). Treatment of HCT-116 cells with G07 at 1.25, 2.5, 5, 10 and 20 µM for 48 h decreased the viability of HCT-116 cells to 94.77 ± 1.55 , 86.91 ± 0.76 , 57.42 ± 2.06 , 32.87 ± 3.33 and 8.86 ± 2.32 , respectively compared with the vehicle control. The IC_{50} value of G07 at 48 h was 6.55 ± 0.16 µM. Thus, G07 at concentrations of 2.5, 5, 10 µM were chosen for further investigation.

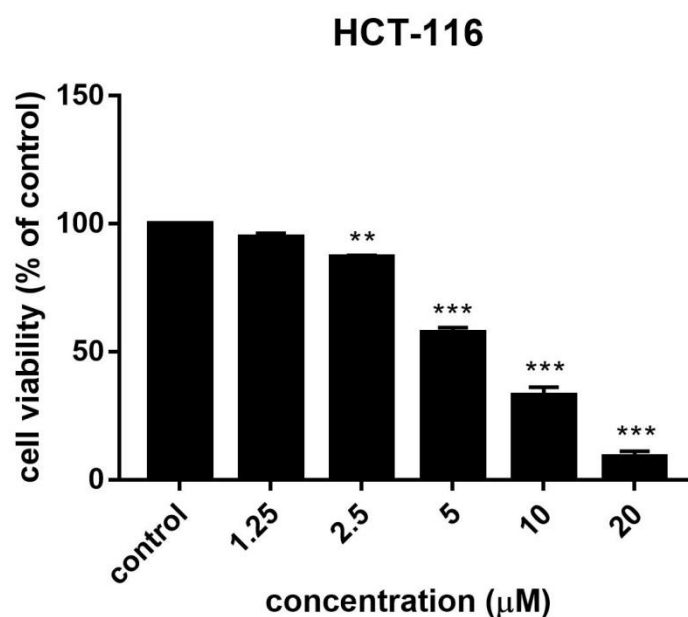


Figure 15 Effect of G07 on the viability of HCT-116 cells. Cells were treated with G07 at 1.25, 2.5, 5, 10 and 20 µM for 48 h. Cell viability was evaluated using MTT assay. Each value is expressed as the mean \pm SEM (n=3). **P<0.01, ***P<0.001 compared with vehicle control (0.2% DMSO).

4.4 Effect of G07 on apoptotic cell death in HCT-116 cells

Most chemotherapeutic agents promote cells to undergo apoptosis (18, 19). To determine the apoptosis-inducing effect of G07, HCT-116 cells were treated with G07, stained with annexin V and propidium iodide (PI) and analyzed by flow cytometry. As shown in Figure 16, the percentages of early and late apoptotic cells were significantly increased after treatment of HCT-116 cells with G07 at 5 and 10 µM, respectively (P<0.05). Flow cytometric analysis revealed that early apoptotic cells significantly increased approximately 7-fold after treatment with 5 µM G07 compared with the vehicle control (P<0.05). In addition, G07 at 10 µM induced HCT-116 cells to undergo late apoptosis approximately 20-fold higher than the vehicle control. Moreover, G07

at this concentration significantly induced necrotic cell death approximately 7 times higher than the vehicle control.

Poly (ADP-ribose) polymerase (PARP) plays an important role in DNA repair and apoptosis and PARP is cleaved by upstream caspases during apoptosis (81). Thus, the protein level of cleaved PARP was determined using western blot. In a good agreement with flow cytometric results, G07 at 5 and 10 μM significantly induced PARP cleavage (Figure 17). Taken together, these results suggest that apoptosis induction is partly responsible for G07-induced cell death in HCT-116 cells.

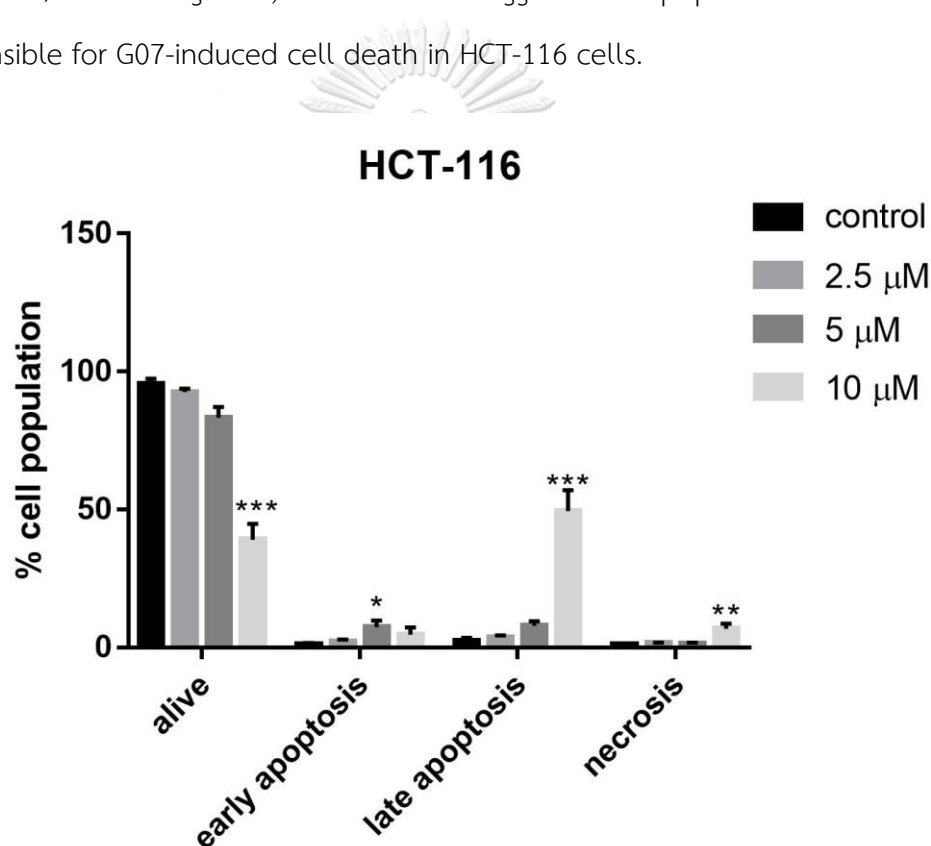


Figure 16 Effect of G07 on apoptosis in HCT-116 cells. Cells were treated with G07 at 2.5, 5 and 10 μM for 24 h. After staining cells with annexin V and PI, the percentages of apoptotic cells or necrotic cells were evaluated using flow cytometry. Each value is expressed as the mean \pm SEM (n=3). * $P < 0.05$, ** $P < 0.01$, *** $P < 0.001$ compared with vehicle control (0.2% DMSO).

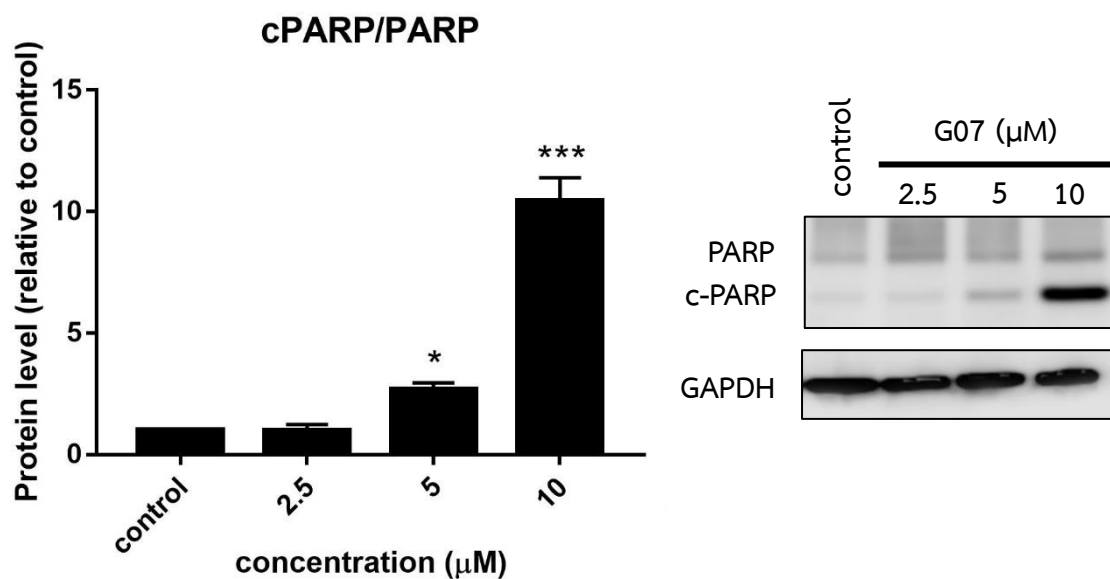


Figure 17 Effect of G07 on PARP cleavage in HCT-116 cells. Cells were treated with G07 at 2.5, 5 and 10 μM for 24 h. The protein levels were evaluated using western blot. Representative immunoblots are shown in the right panel. The values are shown as fold change relative to the vehicle control. Each value is expressed as the mean \pm SEM (n=3). *P<0.05, ***P<0.001 compared with vehicle control (0.2% DMSO).

4.5 Effect of G07 on the expression of Bcl-2 family proteins in HCT-116 cells

Chemotherapeutic agents mainly induce cells to undergo intrinsic apoptosis which is regulated by Bcl-2 family proteins (18, 19). Therefore, the expression of pro-apoptotic proteins, Bak and Bax, and anti-apoptotic proteins, Bcl-2 and Bcl-xl were analyzed. Cells were treated with 2.5, 5, 10 μM of G07 for 24 h and the levels of Bcl-2 family proteins were determined using western blot. As shown in Figure 18A and 18B, treatment with G07 did not alter the expression of Bak and Bax proteins. However, it should be noted that G07 significantly decreased the levels of Bcl-2 protein in a concentration-dependent manner. The Bcl-2 protein levels were decreased by approximately 30%, 40% and 50% compared with the vehicle control after treatment with G07 at 2.5, 5 and 10 μM , respectively (Figure 19A, P<0.05). Similarly, the expression

of Bcl-xl was significantly down-regulated to 75% of the control after treatment with G07 at 10 μM (Figure 19B, $P < 0.05$). Taken together, these results suggest that G07 induces apoptosis by downregulating the expression of anti-apoptotic proteins, Bcl-2 and Bcl-xl, in HCT-116 cells.

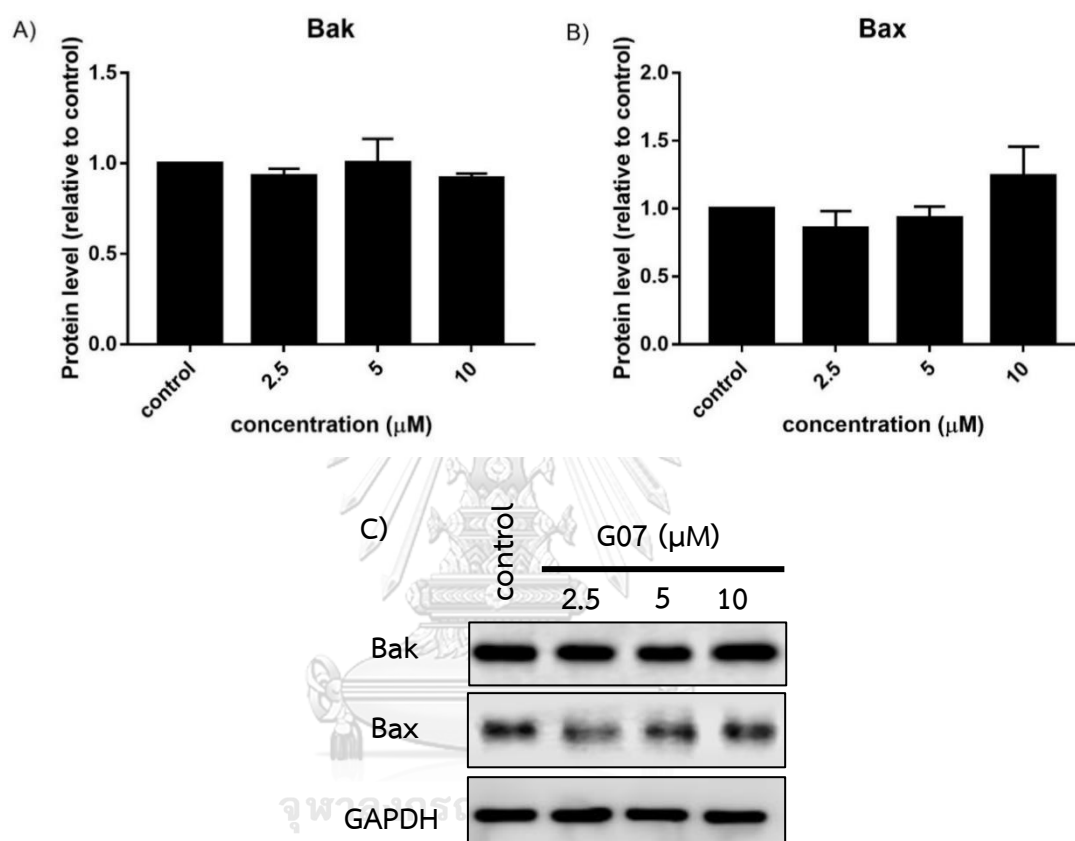


Figure 18 Effect of G07 on the expression of pro-apoptotic Bcl-2 family proteins in HCT-116 cells. Cells were treated with G07 at 2.5, 5 and 10 μM for 24 h. The levels of pro-apoptotic proteins, including A) Bak and B) Bax were evaluated using western blot. C) Representative immunoblots for Bak and Bax. The values are shown as fold change relative to the vehicle control. Each value is expressed as the mean \pm SEM ($n=3$).

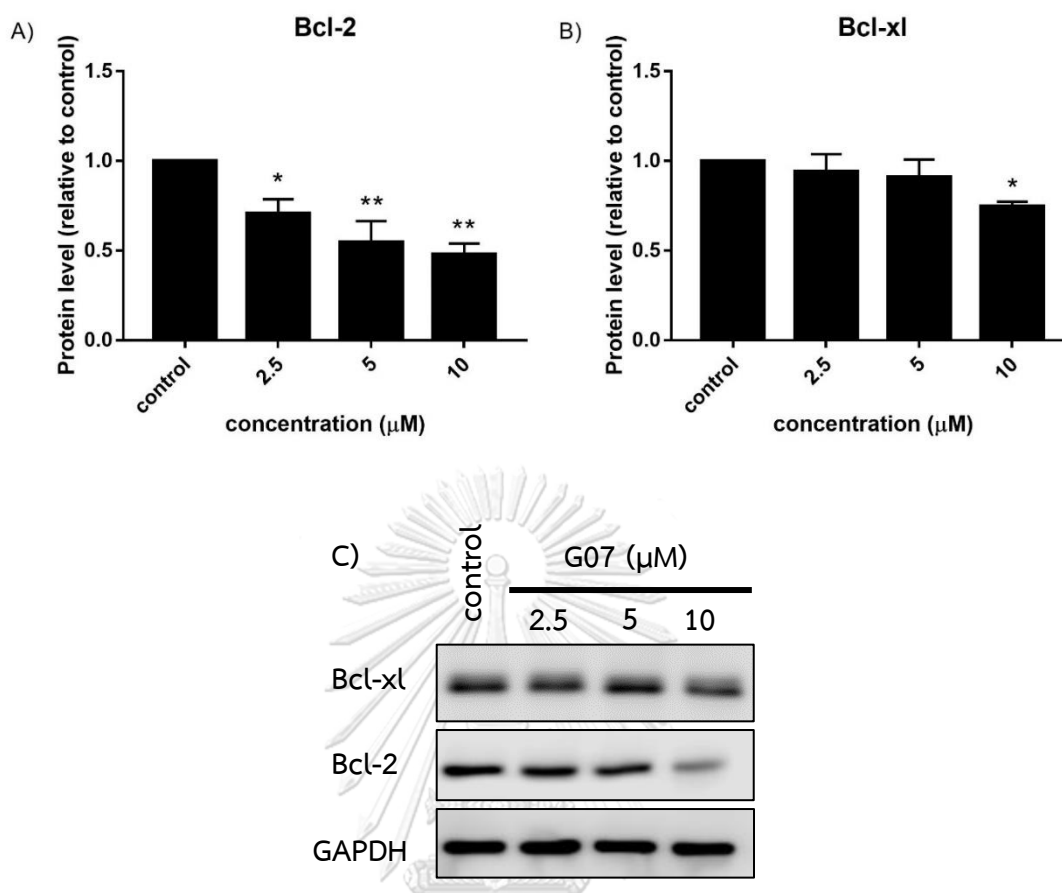


Figure 19 Effect of G07 on the expression of anti-apoptotic Bcl-2 family proteins in HCT-116 cells. Cells were treated with G07 at 2.5, 5 and 10 μM for 24 h. The levels of anti-apoptotic proteins, including A) Bcl-2 and B) Bcl-xl were evaluated using western blot. C) Representative immunoblots for Bcl-xl and Bcl-2. The values are shown as fold change relative to the vehicle control. Each value is expressed as the mean \pm SEM (n=3). *P<0.05, **P<0.01 compared with the vehicle control (0.2%DMSO).

4.6 Effect of G07 on ROS generation in HCT-116 cells

Several studies reported that many anticancer agents exhibited anticancer activity through ROS production (14, 15). Thus, the effect of G07 on ROS production in HCT-116 cells was evaluated. Cells were exposed with 2.5, 5, and 10 μM of G07 or 200 μM of H_2O_2 (positive control) for 1 h and ROS levels were measured using the DCFH-DA assay. As illustrated in Figure 20A, G07 significantly induced ROS production in HCT-

HCT-116 cells in a concentration-dependent manner ($P < 0.05$). The levels of ROS in HCT-116 cells treated with G07 at 2.5, 5, 10 μM and 200 μM of H_2O_2 were increased from 100% to approximately 120%, 140%, 180% and 200% of the vehicle control, respectively. To determine whether ROS generation is involved in the cytotoxic effect of G07, the cells were treated with 5 mM of *N*-acetylcysteine (NAC), a ROS scavenger, for 2 h followed by G07 for 24 h. Cell viability was determined using MTT assay. The results in Figure 20B indicated that NAC could prevent G07-induced cell death. Pretreatment with NAC significantly increased the viability of HCT-116 cells by 1.3, 1.4 and 3.8 folds when compared with the viability of the cells treated with G07 alone at 2.5, 5 and 10 μM , respectively ($P < 0.001$). Taken together, these results suggest that cytotoxicity of G07 is partly mediated via ROS generation.



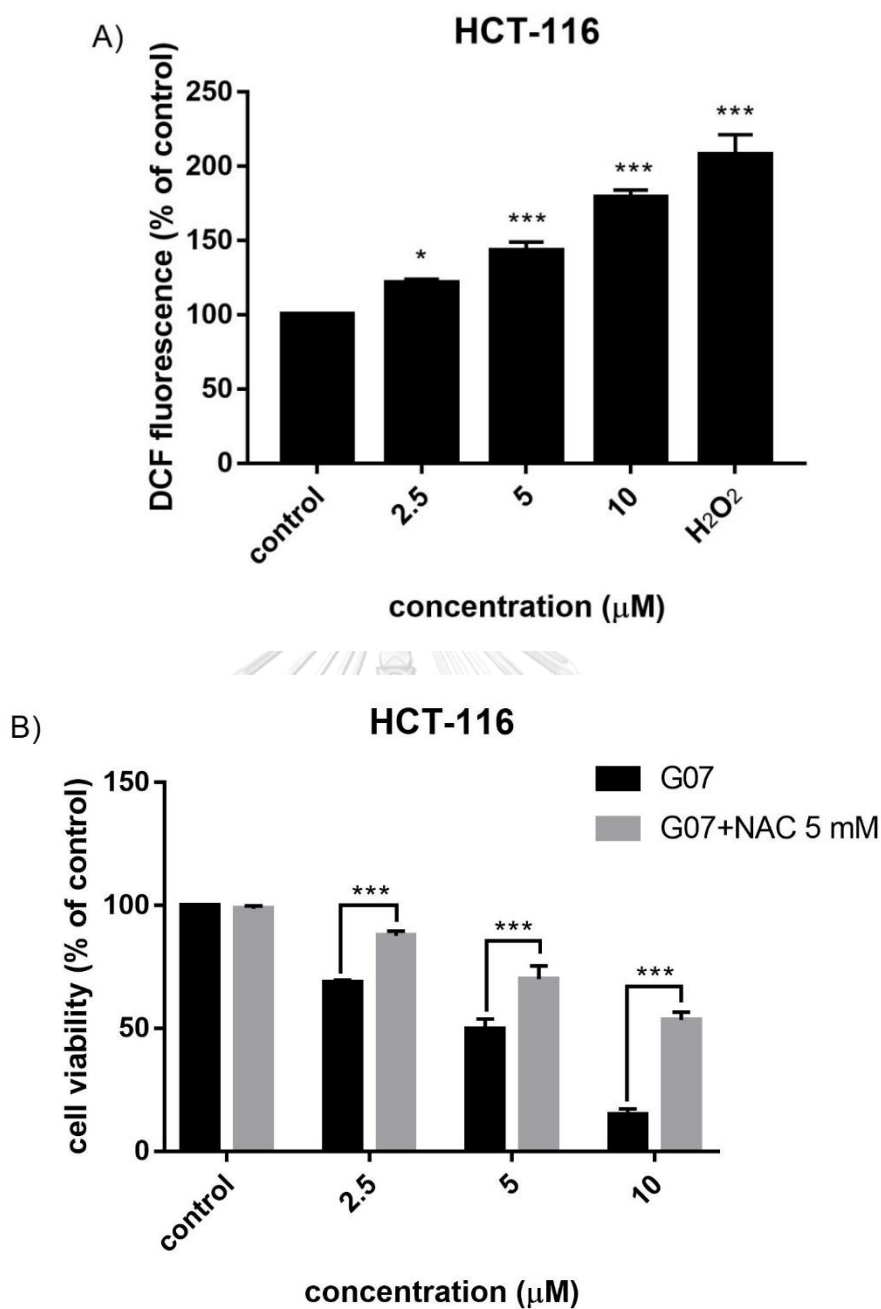


Figure 20 Effect of G07 on ROS generation in HCT-116 cells. A) Cells were treated with G07 at 2.5, 5, 10 μM and 200 μM of H₂O₂ for 1 h. The levels of ROS generation were evaluated using DCFH-DA assay. B) Cells were treated with or without NAC and then treated with G07 for 24 h. Cell viability was determined using MTT assay. Each value is expressed as the mean \pm SEM (n=3). * P<0.05, *** P<0.001 compared with the vehicle control (0.2% DMSO).

4.7 Generation of ROS mediates G07-induced apoptosis in HCT-116 cells

Excessive ROS can induce oxidative stress which in turn activate intrinsic apoptotic machinery, leading to apoptotic cell death (11, 82). Thus, to determine whether ROS generation is necessary for apoptosis-inducing effects of G07 in HCT-116 cells. Cells were pre-treated with or without 5 mM of NAC for 1 h followed by G07 at 2.5, 5 and 10 μ M for 24 h. After staining cells with annexin V/PI, flow cytometry analysis was performed. As shown in Figure 21, NAC prevented apoptosis in HCT-116 cells. Pretreatment with NAC significantly decreased the percentages of G07-induced apoptotic cells at 5 and 10 μ M G07 treatment approximately 2 and 3 folds, respectively ($P < 0.05$), suggesting that G07-induced apoptosis is partly associated with ROS generation.



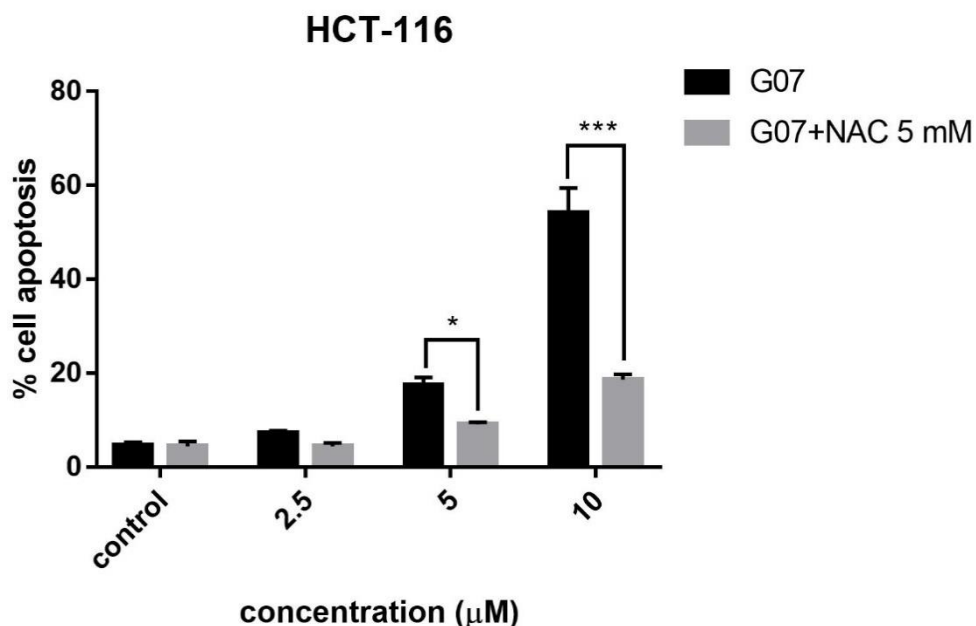


Figure 21 Effect of ROS in G07-induced apoptosis in HCT-116 cells. Cells were treated with or without 5 mM of NAC for 1 h and then treated with G07 at 2.5, 5 and 10 μM for 24 h. After staining cells with annexin V and PI, the percentages of apoptotic cells or necrotic cells were evaluated using flow cytometry. Each value is expressed as the mean \pm SEM (n=3). *P<0.05, ***P<0.001 compared with the vehicle control (0.2% DMSO).

4.8 Effect of G07 on MAPK and PI3K/AKT signaling pathways in HCT-116 cells

MAPK and PI3K/AKT signaling pathways are involved in several cellular functions including cell growth, differentiation, development and apoptosis. It is well known that targeting these two pathways has become effective approaches for CRC treatment (63, 69). Therefore, the effects of G07 on the expression of MAPK and PI3K/AKT signaling proteins including, ERK1/2, p-ERK1/2, AKT and p-AKT were examined by western blotting. As shown in Figure 22A, the expression of phosphorylated ERK1/2 was significantly decreased by approximately 40% after treatment with 10 μM G07 (P<0.01). Furthermore, G07 at 10 μM significantly inhibited the phosphorylation of AKT.

Expression ratio of p-AKT/AKT was decreased to 70% of the vehicle control (Figure 22B, $P < 0.05$). Taken together, these results suggest that cytotoxicity of G07 may be mediated via inhibition of both ERK1/2 and PI3K/AKT signaling pathways in HCT-116 cells.



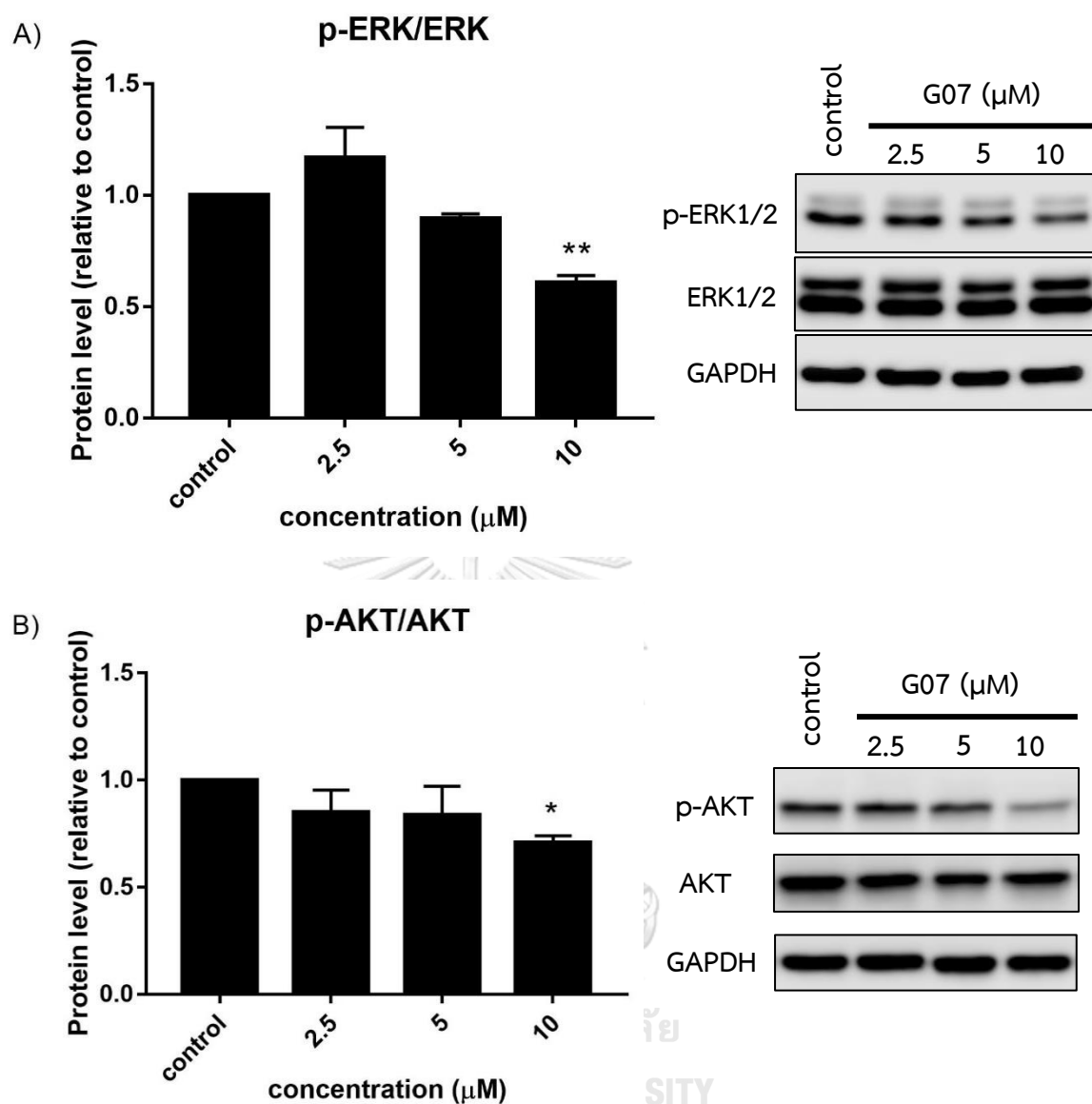


Figure 22 Effect of G07 on the expression of ERK1/2 and PI3K/AKT signaling proteins in HCT-116 cells. Cells were treated with G07 at 2.5, 5 and 10 μM for 24 h. The levels of proteins were evaluated using western blot. The expression ratios of A) phospho-ERK1/2 and total-ERK1/2 B) phospho-AKT and total-AKT were quantified. Representative immunoblots are shown in the right panel. The values are shown as fold change relative to the vehicle control. Each value is expressed as the mean \pm SEM (n=3). *P<0.05 and **P<0.01 compared with the vehicle control (0.2% DMSO).

4.9 Effect of G07 on viability of HT-29 cells

The tumor suppressor p53 plays a critical role in cell cycle arrest, cell senescence and apoptosis (83, 84). Mutation of p53 is commonly found in human colorectal cancer and is also associated with drug resistance (39, 83-85). Thus, compound that remains effective in p53-mutant cancer cells is urgently needed. In the present study, cytotoxicity of G07 was determined in p53 mutant cells, HT-29 cells. Cells were incubated with various concentrations of G07. After 48 h, cell viability was determined by MTT assay. As illustrated in Figure 23, G07 significantly decreased the viability of HT-29 cells in a concentration-dependent manner ($P < 0.01$). The percentages of viable HT-29 cells, which were exposed to G07 at 1.25, 2.5, 5, 10 and 20 μM for 48 h, decreased to 88.83 ± 2.58 , 84.45 ± 1.83 , 79.30 ± 1.88 , 42.02 ± 4.68 and $5.29 \pm 0.23\%$, of the vehicle control, respectively. The IC_{50} values of G07 at 48 h was $8.22 \pm 0.36 \mu\text{M}$. Thereby, the concentrations of G07 at 5, 10 and 20 μM were chosen for further investigation.

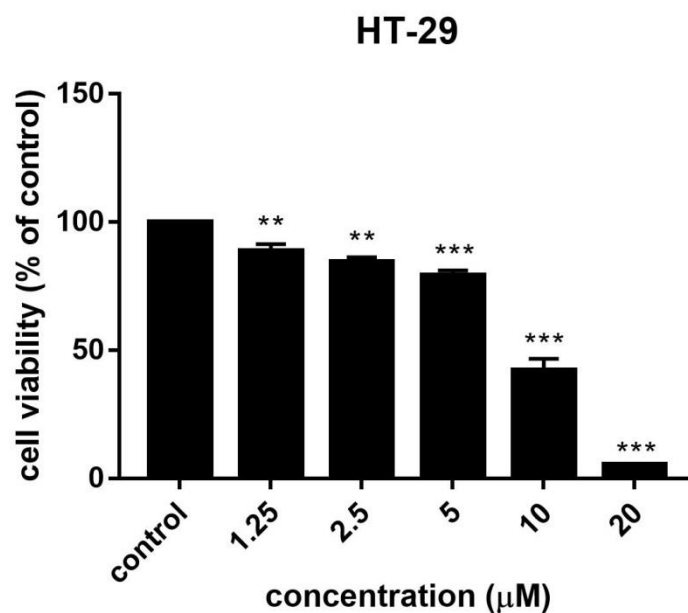


Figure 23 Effect of G07 on the viability of HT-29 cells. Cells were treated with G07 at 1.25, 2.5, 5, 10 and 20 μM for 48 h. Cell viability was evaluated using MTT assay. Each value is expressed as the mean \pm SEM (n=3). **P<0.01, ***P<0.001 compared with vehicle control (0.2% DMSO).

4.10 Effect of G07 on apoptotic cell death in HT-29 cells

To determine whether cytotoxicity of G07 was due to apoptosis in HT-29 cells, cells were treated with G07 at 5, 10 and 20 μM for 24 h. The treated cells were stained with annexin V and PI and analyzed by flow cytometry. As shown in Figure 24, HT-29 cells underwent early and late apoptosis after treatment with G07 at 20 μM (P<0.05). The percentages of early and late apoptotic cells were increased approximately 2-fold and 6-fold of the vehicle control respectively, (P<0.05). Additionally, necrotic cells were detected after treatment with G07 at 20 μM.

In a good agreement with flow cytometric results, western blot analysis demonstrated that treatment with 20 μM of G07 significantly induced PARP cleavage

(Figure 25, $P < 0.01$). Taken together, these results suggest that cytotoxicity of G07 is partly mediated via apoptosis induction in HT-29 cells.

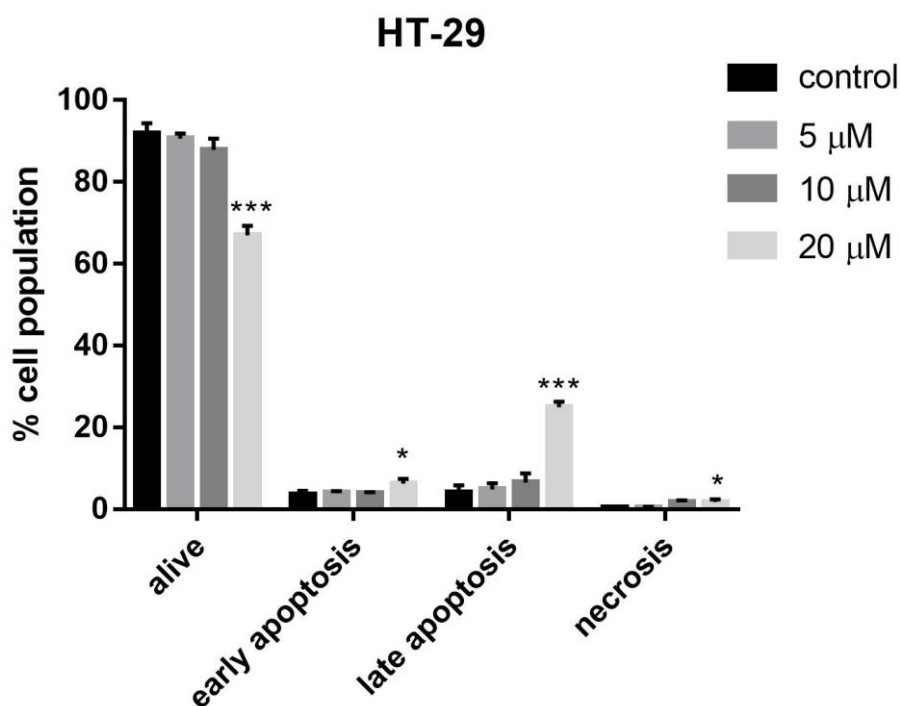


Figure 24 Effect of G07 on apoptosis in HT-29 cells. Cells were treated with G07 at 5, 10 and 20 μM for 24 h. After staining cells with annexin V and PI, the percentages of apoptotic cells or necrotic cells were evaluated using flow cytometry. Each value is expressed as the mean \pm SEM ($n=3$). * $P < 0.05$, *** $P < 0.001$ compared with vehicle control (0.2% DMSO).

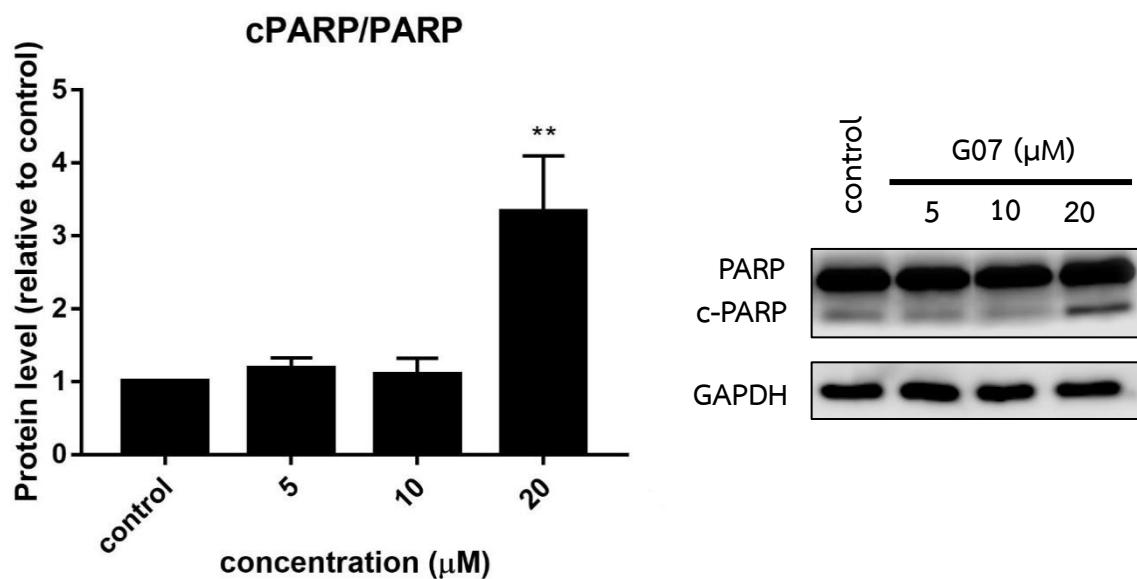
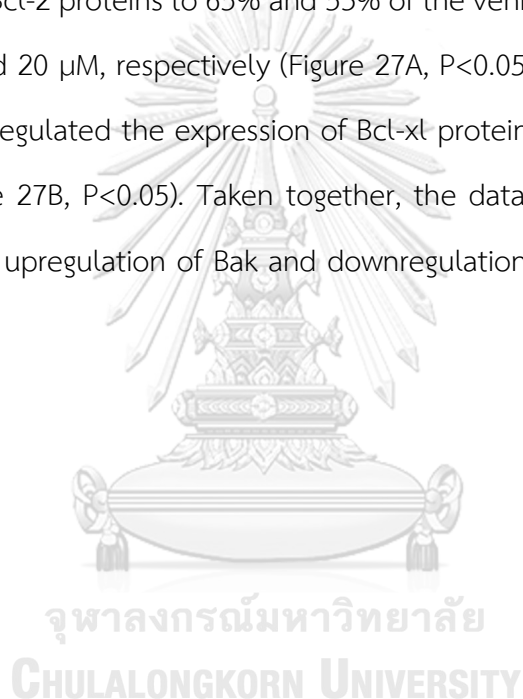


Figure 25 Effect of G07 on PARP cleavage in HT-29 cells. Cells were treated with G07 at 5, 10 and 20 μM for 24 h. The protein levels were evaluated using western blot. Representative immunoblots are shown in the right panel. The values are shown as fold change relative to the vehicle control. Each value is expressed as the mean \pm SEM (n=3). *P<0.05, **P<0.01 compared with vehicle control (0.2% DMSO).

4.11 Effect of G07 on expression of Bcl-2 family proteins in HT-29 cells

In order to determine whether Bcl-2 family members are involved in G07-induced apoptosis in p53 mutant HT-29 cells. Cells were incubated with G07 at 5, 10 and 20 μ M for 24 h and the expression of Bcl-2 family proteins was determined by western blots. As illustrated in Figure 26A, the protein level of Bak, was significantly increased after treatment with 20 μ M of G07 ($P < 0.05$). Conversely, it did not alter the expression of Bax protein (Figure 26B). In addition to Bak, G07 significantly suppressed the expression of Bcl-2 proteins to 65% and 53% of the vehicle control after treatment with G07 at 10 and 20 μ M, respectively (Figure 27A, $P < 0.05$). Moreover, 20 μ M of G07 significantly downregulated the expression of Bcl-xl protein by approximately 40% of the control (Figure 27B, $P < 0.05$). Taken together, the data suggest that G07 induces apoptosis through upregulation of Bak and downregulation of Bcl-2 and Bcl-xl in HT-29 cells.



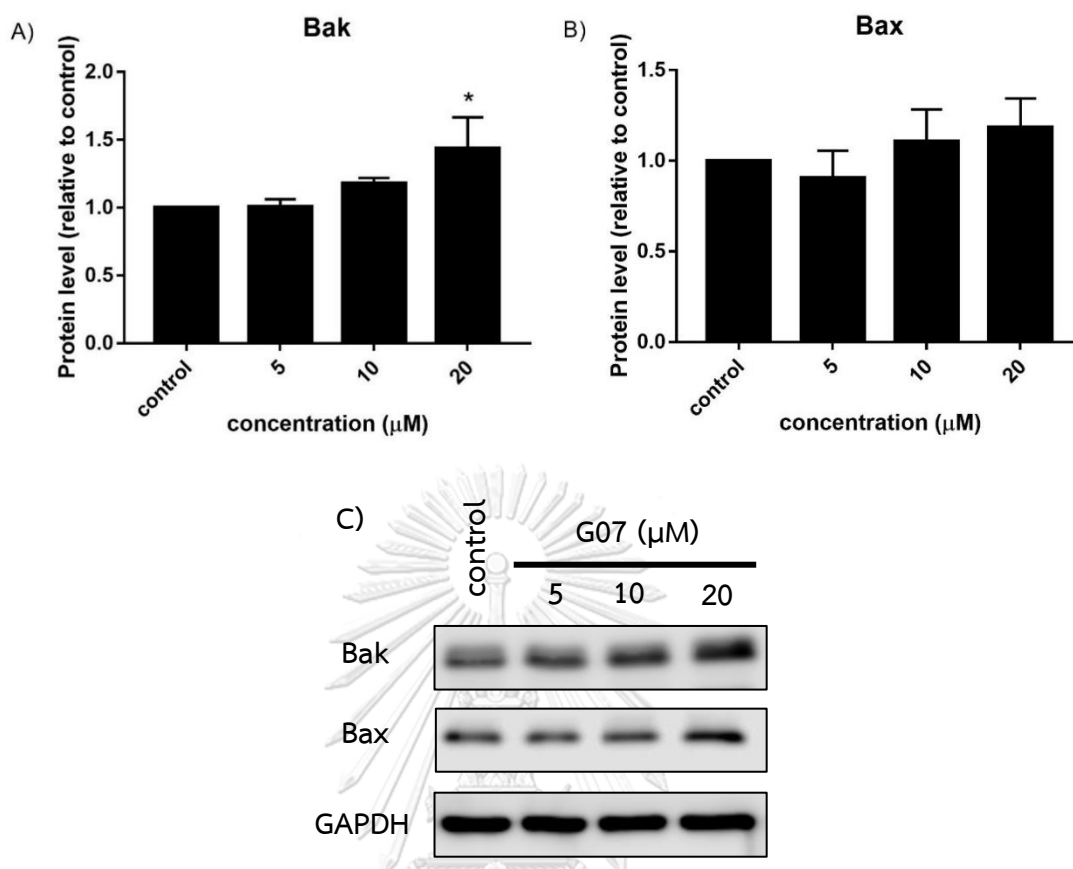


Figure 26 Effect of G07 on the expression of pro-apoptotic Bcl-2 family proteins in HT-29 cells. Cells were treated with G07 at 5, 10 and 20 μM for 24 h. The levels of pro-apoptotic proteins including, A) Bak and B) Bax were evaluated using western blot. C) Representative immunoblots for Bak and Bax. The values are shown as fold change relative to the vehicle control. Each value is expressed as the mean \pm SEM (n=3). *P<0.05 compared with vehicle control (0.2% DMSO).

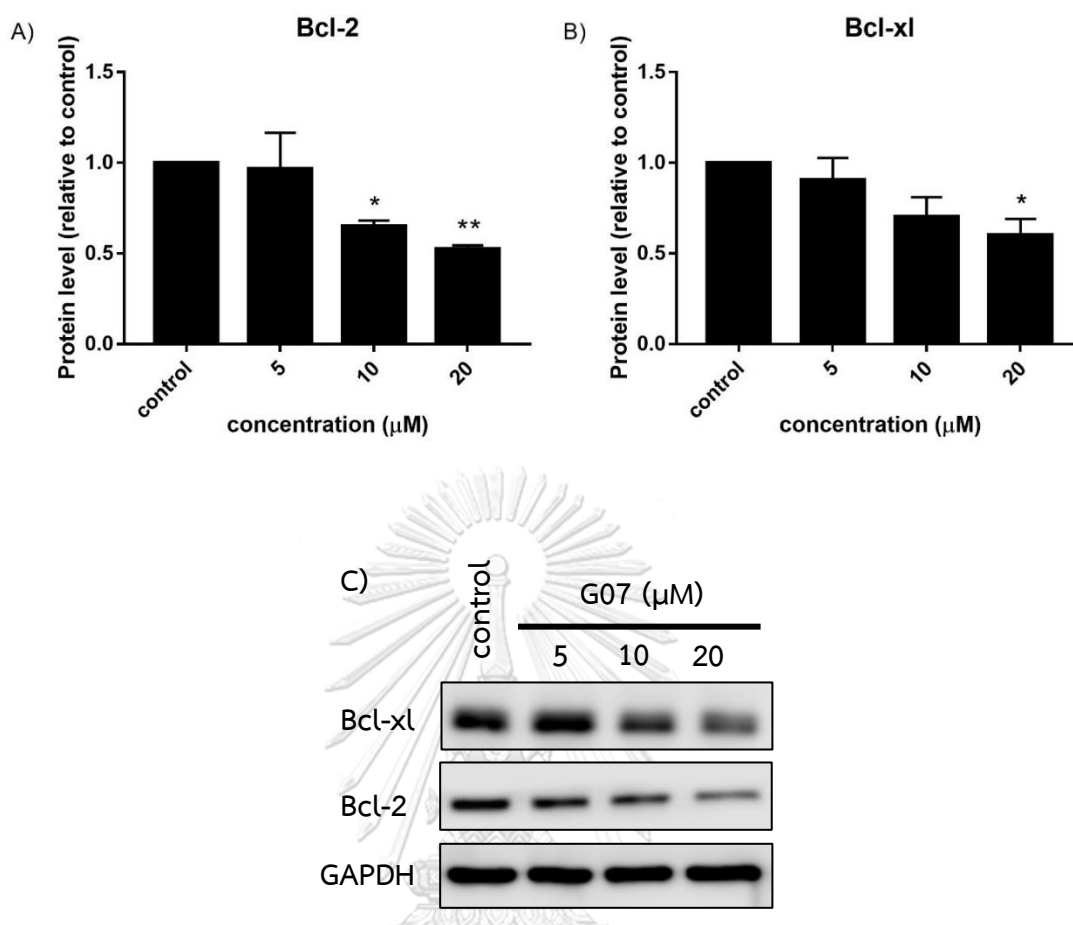


Figure 27 Effect of G07 on the expression of anti-apoptotic Bcl-2 family proteins in HT-29 cells. Cells were treated with G07 at 5, 10 and 20 μM for 24 h. The levels of anti-apoptotic proteins including, A) Bcl-2 and B) Bcl-xl were evaluated using western blot. C) Representative immunoblots for Bcl-xl and Bcl-2. The values are shown as fold change relative to the vehicle control. Each value is expressed as the mean \pm SEM (n=3). *P<0.05, **P<0.01 compared with vehicle control (0.2% DMSO).

4.12 Effect of G07 on ROS generation in HT-29 cells

To investigate the effect of G07 on ROS generation in HT-29 cells, the cells were incubated with G07 at 5, 10 and 20 μM or H_2O_2 at 200 μM for 1 h and ROS levels were measured using DCFH-DA assay. As shown in Figure 28A, 10 and 20 μM of G07 and 200 μM of H_2O_2 markedly increased ROS levels to approximately 150%, 240% and 190%, respectively when compared with the vehicle control ($P < 0.001$). MTT assay results showed that NAC significantly prevented G07-induced cell death by 1.3, 1.4 and 3.6 folds when compared with treatment with G07 alone at 5, 10 and 20 μM , respectively (Figure 28B, $P < 0.001$), suggesting that ROS generation is partly involved in the cytotoxicity of G07.



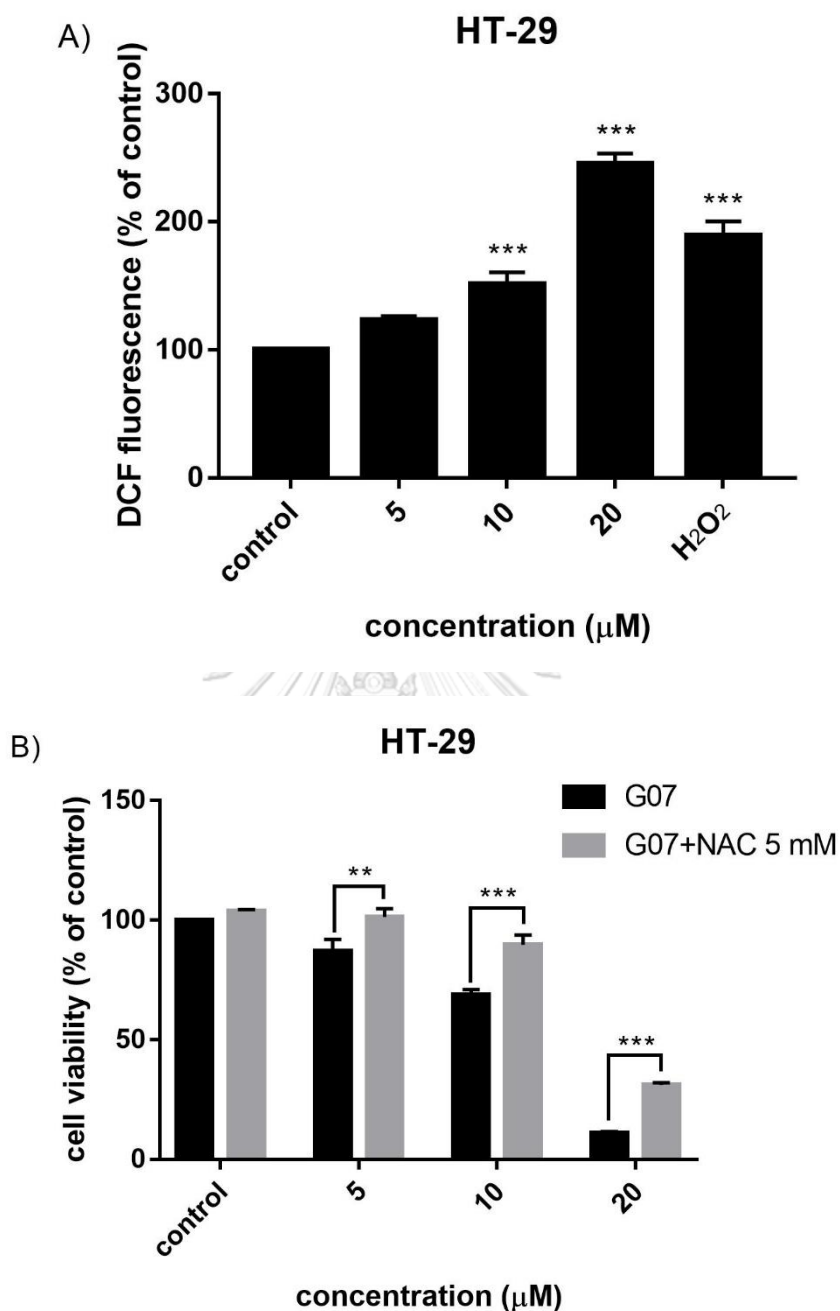


Figure 28 Effect of G07 on ROS generation of HT-29 cells. A) Cells were treated with G07 at 5, 10 and 20 μM or H₂O₂ at 200 μM for 1 h. The levels of ROS generation were evaluated using DCFH-DA assay. B) Cells were treated with or without NAC and then treated with G07 for 24 h. Cell viability was determined by using MTT assay. Each value is expressed as the mean \pm SEM (n=3). ** P<0.01, *** P<0.001 compared with the vehicle control (0.2% DMSO).

4.13 Generation of ROS mediates G07-induced apoptosis in HT-29 cells

To determine whether the apoptosis-inducing effect of G07 is mediated through ROS generation in HT-29 cells. Cells were treated with or without 5 mM of NAC for 1 h followed by G07 at 5, 10 and 20 μM for 24 h. After staining cells with annexin V/PI, flow cytometry was evaluated. As illustrated in Figure 29, G07 at 20 μM significantly induced apoptosis and pretreatment with 5 mM NAC markedly decreased the percentages of apoptotic cells by 2.4-fold ($P < 0.001$). These results suggested that ROS generation is partly involved in G07-induced apoptosis in HT-29 cells.

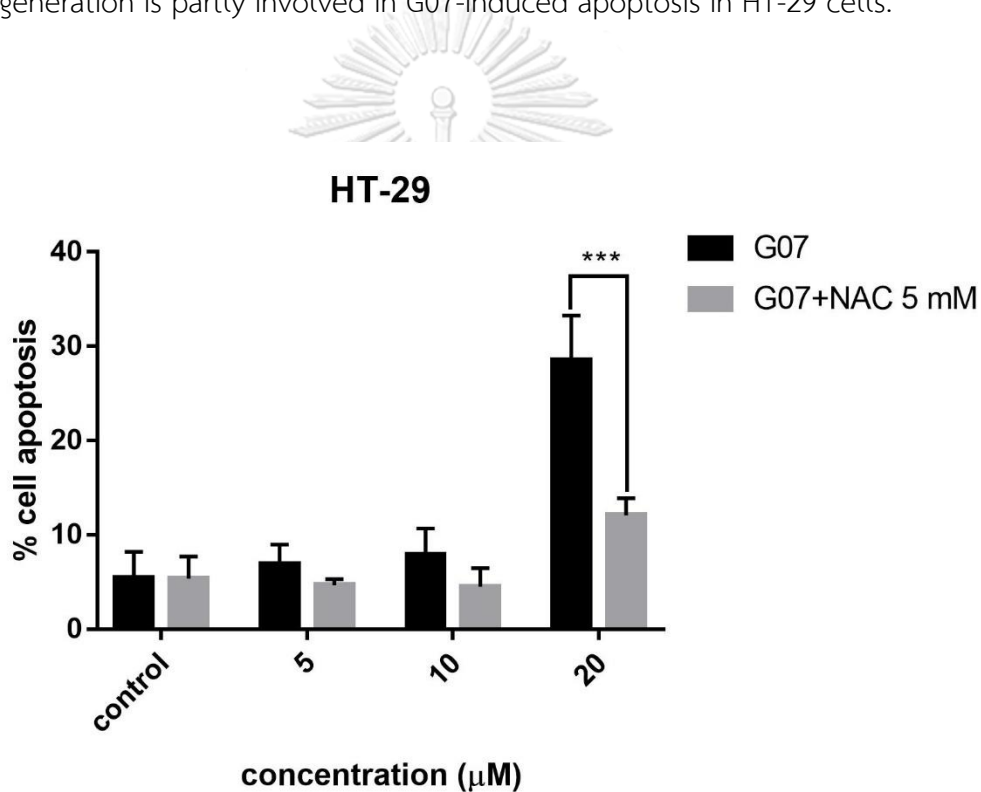
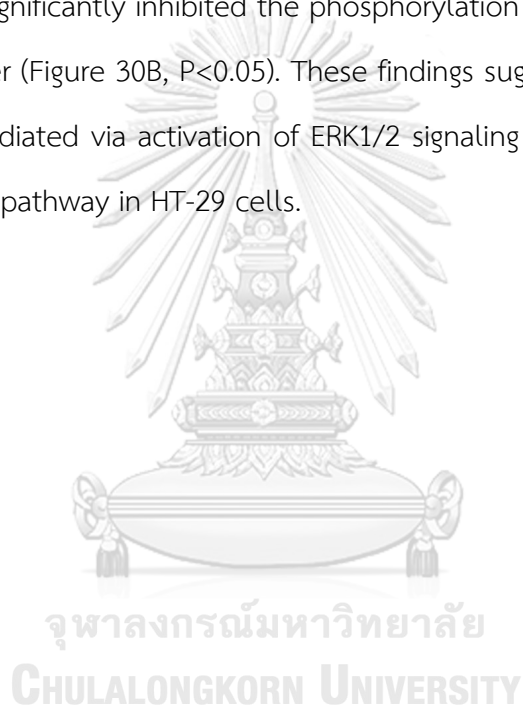


Figure 29 Effect of ROS on G07-induced apoptosis in HT-29 cells. Cells were treated with or without 5 mM of NAC for 1 h and then treated with G07 at 5, 10 and 20 μM for 24 h. After staining cells with annexin V and PI, the percentages of apoptotic cells or necrotic cells were evaluated using flow cytometry. Each value is expressed as the mean \pm SEM ($n=3$). *** $P < 0.001$ compared with vehicle control (0.2% DMSO).

4.14 Effect of G07 on MAPK and PI3K/AKT signaling pathways in HT-29 cells

In order to investigate the mechanism(s) underlying G07-induced cell death, the effects of G07 on MAPK and PI3K/AKT signaling pathways in HT-29 cells were evaluated. The expression of p-ERK1/2, ERK1/2, p-AKT and AKT proteins was determined using western blot. The results showed that 20 μ M of G07 markedly induced the phosphorylation of ERK1/2 (Figure 30A, $P < 0.001$). The p-ERK1/2/total ERK1/2 ratio was increased approximately 7-fold above the vehicle control. On the other hand, G07 significantly inhibited the phosphorylation of AKT in a concentration-dependent manner (Figure 30B, $P < 0.05$). These findings suggest that G07-induced cell death may be mediated via activation of ERK1/2 signaling pathway and inhibition of PI3K/AKT signaling pathway in HT-29 cells.



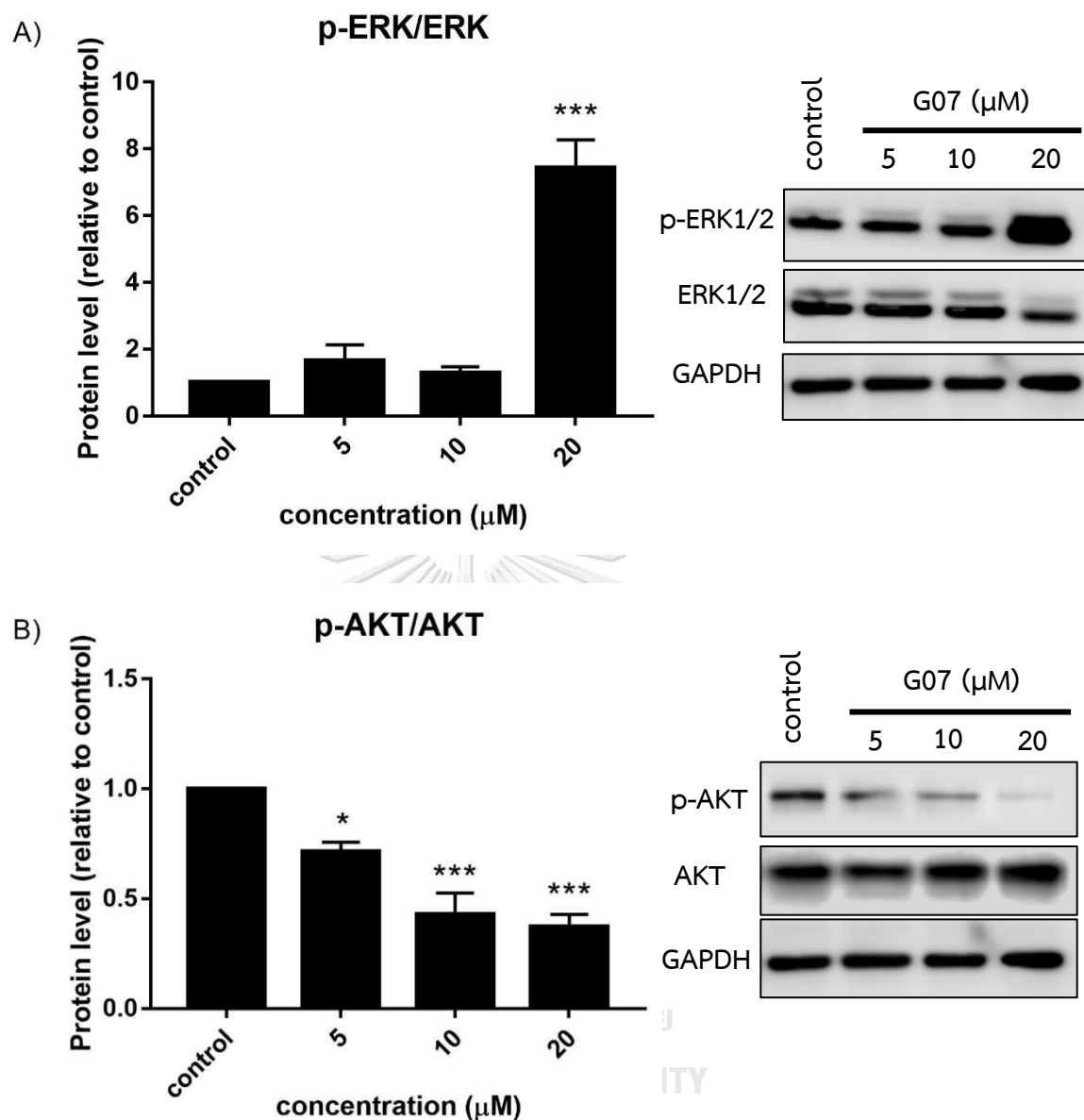


Figure 30 Effect of G07 on the expression of ERK1/2 and PI3K/AKT signaling proteins in HT-29 cells. Cells were treated with G07 at 5, 10 and 20 μM for 24 h. The levels of protein were evaluated using western blot. The expression ratios of A) phospho-ERK1/2 and total-ERK1/2 B) phospho-AKT and total-AKT were quantified. Representative immunoblots are shown in the right panel. The values are shown as fold change relative to the vehicle control. Each value is expressed as the mean \pm SEM (n=3). *P<0.05 and ***P<0.001 compared with vehicle control (0.2% DMSO).

CHAPTER V

DISCUSSION AND CONCLUSION

CRC is a major cause of cancer-related death worldwide. Nowadays, treatment options of CRC are surgery, radiotherapy, chemotherapy and targeted therapy (3, 4). Chemotherapy is one of the most effective and potent strategy to treat cancer. However, its application for CRC treatment has been limited due to acquired drug resistance (86, 87) and several serious side effects (47-49). Although targeted drugs do not affect the body the same way as chemotherapeutic drugs, they still do cause side effects. And many targeted cancer drugs can be extremely expensive (88). Thus, potent novel anticancer therapeutic agents with low toxicity are urgently needed.

Mansonone is a naphthoquinone-containing compound, isolated from *Mansonia gagei* Drumm, a Thai traditional plant which is locally used as an antidepressant, antiemetic, cardiac stimulant and refreshment agent (20, 74). It was reported that mansonone E and F exhibited anticancer effect against various cancer cell lines including melanoma (A375-S2), cervical cancer (HeLa), breast cancer (MCF-7), lymphoma (U937), cervical cancer (HeLa), colorectal cancer (HT-29), oral cavity cancer (KB) and leukemia cell lines (HL60, K562, THP-1 and U937) (23-25). However, the anticancer effect of mansonone G (MG) against CRC cells has not been reported. In this study, the anticancer effects of MG and its ten semi-synthetic derivatives were investigated on two human CRC cell lines, HCT-116 cells carrying p53 wild-type and HT-29 cells carrying p53 mutant. The results showed that MG and its derivatives inhibited the growth of the two cell lines in a concentration-dependent manner. Notably, MG derivatives including G01, G02, G03, G04, G05, G06, G07, G08, G09 and G10 were more toxic to cancer cells than the parent compound. These findings were consistent with the finding of Hairani et al., 2016 that ether analogues of MG exerted higher antibacterial activity than the parent MG (20). It was suggested that increasing

alkyl chain length of ether analogues of MG made the compounds more hydrophobic, which may facilitate the access to bacterial cell wall, resulting in higher antibacterial activity (20). Therefore, it is possible that increasing the number of carbon units in the alkyl side chain contributes to an increasing cytotoxicity of MG derivatives toward human CRC cells. Since G07 exhibited its cytotoxicity more specifically on cancer cells than normal cells (Figure 13 & 14), its anticancer activity and the underlying mechanisms were further investigated. Notably, G07 was more toxic to p53 wild-type HCT-116 cells ($IC_{50}=6.55\pm 0.16 \mu M$) than p53 mutant HT-29 cells ($IC_{50}=8.22\pm 0.36 \mu M$). Previous studies reported that p53 mutant cells are less susceptible to cytotoxicity of chemotherapeutic agents than p53 wild-type cells (84, 89). Furthermore, mutations of p53 in cancer patients are associated with the drug resistance and poor clinical outcome (38). Thus, it is possible that p53 plays an important role in sensitivity of CRC cells to the cytotoxic activity of G07.

Several chemotherapy agents as well as naphthoquinone-containing compounds induce cancer cells to undergo apoptosis (16, 90-93). A previous study demonstrated that the apoptosis-inducing effect of mansonone E in human cervical cancer cells is mediated through upregulation of Bax and downregulation of Bcl-2 and Bcl-xl (23). In this study, G07 could induce apoptosis in both HCT-116 and HT-29 cells (Figures 16 & 24). Western blot analysis revealed that G07 downregulated the expression of Bcl-2 and Bcl-xl proteins in HCT-116 cells (Figure 19) whereas upregulation of Bak and downregulation of Bcl-2 and Bcl-xl were observed in G07-treated HT-29 cells (Figures 26 & 27). Taken together, these results suggest that G07-induced apoptosis is mediated through modulation of Bcl-2 family proteins in HCT-116 and HT-29 cells. It is commonly known that caspase-mediated apoptotic cell death is accomplished through the cleavage of several key proteins required for cellular functions and cell survival. PARP is one of the several substrates of caspases (25-27).

The present study demonstrated that G07 induced PARP cleavage in both HCT-116 and HT-29 cells (Figures 17 & 25), suggesting that apoptosis-inducing effect of G07 may be associated with the caspase activation and the PARP cleavage. Notably, this study found that apoptosis-inducing effect of G07 was more pronounced in HCT-116 cells than HT-29 cells. The results of this study were in agreement with previous studies that cells expressing mutant p53 were more resistant to irradiation, doxorubicin and cisplatin-induced apoptosis than cells expressing wild-type p53 (94, 95).

Compared to the normal cells, cancer cells have higher metabolism and oxidative stress, suggesting that higher levels of ROS can be generated in cancer cells than normal cells. Therefore, the accumulation of ROS can be a strategy for selectively killing cancer cells (11). Previously, naphthoquinone-containing compounds such as curcumin, plumbagin, shikonin and lawsone were shown to induce apoptosis via ROS generation in various cancer cell lines (96). Similarly, the present study found that G07 induced ROS production in CRC cells in a concentration-dependent manner (Figures 20A & 28A) and NAC could prevent G07-induced cell death in HCT-116 and HT-29 cells (Figures 20B & 28B). Moreover, pretreatment with 5 mM NAC could abolish G07-induced apoptosis in both cell lines (Figures 21 & 29). Taken together, these results suggest that ROS generation is involved in cytotoxic and apoptosis-inducing effects of G07 in CRC cells. It was reported that ROS act as upstream signal that triggers p53 activation, leading cells to apoptosis induction (97, 98). Conversely, ROS was found to be an important mediator for apoptosis induction in p53-independent pathway (99-101). It was reported that doxorubicin induced apoptosis through ROS accumulation in p53-null human osteosarcoma Saos-2 cells (102). Thus, it is likely that G07 could induce CRC cells to undergo apoptosis via accumulation of ROS irrespective of p53 status. However, the molecular mechanism underlying these observations remains to be elucidated.

MAPK and PI3K/AKT signaling pathways are the central signal transduction mechanisms for controlling cell proliferation, survival, metabolism, motility and apoptosis (103). Constitutive activation of MAPK and PI3K/AKT signaling pathways have been reported to play essential roles in CRC progression, metastasis and drug resistance (104). The proteins associated with these pathways are considered as molecular targets for anticancer drugs. ERK is a major regulator of cell proliferation in CRC (63). Previous study reported that activation of MEK-ERK1/2 pathway promoted tumorigenicity and metastasis in CD133⁺ primary colon cancer cells and the clonogenic growth of CD133⁺ cells was reduced greatly by inhibiting the ERK1/2 activity (105). In addition, it was shown that suppression of ERK1/2 MAPK pathway induces cancer cells to undergo apoptosis through modulation of apoptotic proteins (62). NTDMNQ, 1,4-naphthoquinone, and its derivatives could induce apoptosis via down-regulation of phosphorylated ERK1/2 and accumulation of ROS (92). A recent study also demonstrated that quinalizarin exhibits apoptosis-inducing effect by suppressing ERK phosphorylation in CRC (106). Remarkably, the results in this study revealed that G07 inhibited ERK1/2 phosphorylation in HCT-116 cells (Figure 22A) but induced ERK1/2 phosphorylation in HT-29 cells (Figure 30A). Accumulating evidence has shown that activation of ERK1/2 generally promotes cell survival, but under certain condition, aberrant ERK1/2 activation contribute to enhance apoptosis (62, 107). Gulati AP et al. revealed that TPA-modulated RAS/ERK signaling pathways differently depending on the status of p53 in the cells (108). Moreover, it was shown that piperlongumine induced ERK phosphorylation, leading to cell death in p53 mutant HT-29 cells (109). Similarly, phenethyl Isothiocyanate (PEITC)-induced apoptosis in p53-deficient PC-3 human prostate cell line was mediated via ERK activation and apoptosis-inducing effect of PEITC was abolished in the presence of an ERK1/2 inhibitor (110). Taken together, it is likely that ERK activation may be associated with G07-induced apoptotic cell death in p53-mutant HT-29 cells observed in this study.

In addition to MAPK signaling pathway, PI3K/AKT signaling pathway frequently activated in CRC, suggesting that using an agent targeting this pathway may be an effective strategy for CRC therapy. A previous study demonstrated that ramentaceone, a naphthoquinone derived from *Drosera sp.*, induced apoptosis via inhibition of PI3K/AKT pathway in breast cancer (90). Similarly, furano-1,2-naphthoquinone (FNQ) isolated from *Avicennia marina* inhibited AKT phosphorylation, resulting in cell cycle arrest at G2/M phase and apoptosis in human oral squamous carcinoma cancer cells (111). In addition, acetylshikonin could inhibit PI3K/AKT/mTOR signaling pathway, leading to inhibition of cell proliferation and induction of cell cycle arrest at G0/G1 phase and apoptosis *in vitro* as well as suppression of cancer cell growth *in vivo* (93). These findings are consistent with the results obtained in this study that G07 effectively inhibited AKT phosphorylation in HCT-116 and HT-29 cells (Figures 22B & 30B) in a concentration dependent manner. Thus, it is possible that, in addition to modulation of ERK signaling pathway, anticancer activity of G7 may be mediated through inhibition of PI3K/AKT signaling in CRC cells.

Conclusion

The present study clearly demonstrated that G07, a mansonone G derivative, exerted a potent anticancer activity against two CRC cell lines, p53 wild-type HCT-116 and p53 mutant HT-29. G07 could induce ROS generation, leading to apoptosis in both HCT-116 and HT-29 cells. Western blot analysis revealed that G07 downregulated the expression of Bcl-2 and Bcl-xl proteins in both cells and upregulated the expression of Bak protein in HT-29 cells. Furthermore, G07 downregulated AKT signaling pathway and modulated ERK1/2 signaling pathway by inhibiting ERK1/2 phosphorylation in HCT-116 cells and activating ERK1/2 phosphorylation in HT-29 cells. Taken together, the results from this study suggest that G07 can potentially be developed as a novel anticancer agent. However, the present study only provided the first step of mechanisms underlying the cytotoxic effect of G07 in CRC cell lines carrying wild-type and mutant p53. Further mechanistic studies need to be performed in order to gain more insight into the anticancer activity of G07.

REFERENCES

1. Observatory GC. Colorectal cancer. International agency for research on cancer. 2018:1-2.
2. Imsamran W, Chaiwerawattana A, Wiangnon S, Pongnikorn D, Suwanrungrung K. Hospital-based cancer registry NCI2 2016. National cancer institute. 2016;32:1-94.
3. Deverakonda A. Diagnosis and treatment of colorectal cancer: a review. Research and reviews journal of medical and health sciences. 2016;8(1):1-15.
4. Hammond WA, Swaika A, Mody K. Pharmacologic resistance in colorectal cancer: a review. Therapeutic advances in medical oncology. 2016;8(1):57-84.
5. Dickinson BC, Chang CJ. Chemistry and biology of reactive oxygen species in signaling or stress responses. Nature chemical biology. 2011;7(8):504-11.
6. Liou GY, Storz P. Reactive oxygen species in cancer. Free radical research. 2010;44(5):479-96.
7. Liu H, Liu X, Zhang C, Zhu H, Xu Q, Bu Y, et al. Redox imbalance in the development of colorectal cancer. Journal of cancer. 2017;8(9):1586-97.
8. Schieber M, Chandel NS. ROS function in redox signaling and oxidative stress. Current biology. 2014;24(10):453-62.
9. Sreevalsan S, Safe S. Reactive oxygen species and colorectal cancer. Current colorectal cancer reports. 2013;9(4):350-57.
10. Trachootham D, Alexandre J, Huang P. Targeting cancer cells by ROS-mediated mechanisms: a radical therapeutic approach? Nature review drug discovery. 2009;8(7):579-91.
11. Redza-Dutordoir M, Averill-Bates DA. Activation of apoptosis signalling pathways by reactive oxygen species. Biochimica et biophysica acta. 2016;1863(12):2977-92.
12. Circu ML, Aw TY. Reactive oxygen species, cellular redox systems, and apoptosis. Free radical biology and medicine. 2010;48(6):749-62.
13. Matés JM, Sánchez-Jiménez FM. Role of reactive oxygen species in apoptosis: implications for cancer therapy. The international journal of biochemistry and cell biology. 2000;32(2):157-70.

14. Fang J, Nakamura H, Iyer AK. Tumor-targeted induction of oxystress for cancer therapy. *Journal of drug targeting*. 2007;15(7-8):475-86.
15. Yokoyama C, Sueyoshi Y, Ema M, Mori Y, Takaishi K, Hisatomi H. Induction of oxidative stress by anticancer drugs in the presence and absence of cells. *Oncology letters*. 2017;14(5):6066-70.
16. Zhang L, Yu J. Role of apoptosis in colon cancer biology, therapy, and prevention. *Current colorectal cancer reports*. 2013;9(4):1-14.
17. Yang SY, Sales KM, Fuller B, Seifalian AM, Winslet MC. Apoptosis and colorectal cancer: implications for therapy. *Trends in molecular medicine*. 2009;15(5):225-33.
18. Rudin CM, Thompson CB. Apoptosis and disease: regulation and clinical relevance of programmed cell death. *Annual review of medicine*. 1997;48(1):267-81.
19. Favaloro B, Allocati N, Graziano V, Di Ilio C, De Laurenzi V. Role of apoptosis in disease. *Aging*. 2012;4(5):330-49.
20. Hairani R, Mongkol R, Chavasiri W. Allyl and prenyl ethers of mansonone G, new potential semisynthetic antibacterial agents. *Bioorganic and medicinal chemistry letters*. 2016;26(21):5300-03.
21. Tiew P, Puntumchai A, Kokpol U, Chavasiri W. Coumarins from the heartwoods of *Mansonia gagei* Drumm. *Phytochemistry*. 2002;60(8):773-6.
22. El-Halawany AM, Salah El Dine R, Hattori M. Anti-estrogenic activity of mansonone G and mansorin A derivatives. *Pharmaceutical biology*. 2013;51(8):948-54.
23. Wang D, Xia M, Cui Z, Tashiro S, Onodera S, Ikejima T. Cytotoxic effects of mansonone E and F isolated from *Ulmus pumila*. *Biological and pharmaceutical bulletin*. 2004;27(7):1025-30.
24. Boonsri S, Karalai C, Ponglimanont C, Chantrapromma S, Kanjana-opas A. Cytotoxic and antibacterial sesquiterpenes from *Thespesia populnea*. *Journal of natural products*. 2008;71(7):1173-77.
25. Keyong Ho L. Anti-leukemic and topoisomerase I inhibitory effect of mansonone E isolated from *Ulmus davidiana*. *Journal of medicinal plants research*. 2012;6(24):4091-95.
26. Siegel RL, Miller KD, Jemal A. Cancer statistics, 2017. *A cancer journal for clinicians*. 2017;67(1):7-30.

27. Siegel RL, Miller KD, Fedewa SA, Ahnen DJ, Meester RGS, Barzi A, et al. Colorectal cancer statistics, 2017. *A cancer journal for clinicians*. 2017;67(3):177-93.
28. Davies RJ, Miller R, Coleman N. Colorectal cancer screening: prospects for molecular stool analysis. *Nature reviews cancer*. 2005;5(3):199-209.
29. Amersi F, Agustin M, Clifford Y. Colorectal cancer: epidemiology, risk factors and health services. *Clinics in colon and rectal surgery*. 2005;18:133-40.
30. Kuipers EJ, Grady WM, Lieberman D, Seufferlein T, Sung JJ, Boelens PG, et al. Colorectal cancer. *Nature reviews disease primers*. 2015;1:1-25.
31. Siegel R, Jemal A. Colorectal cancer facts and figures 2017-2019. *American cancer society*. 2017;9:1-36.
32. Kolligs FT. Diagnostics and epidemiology of colorectal cancer. *Visceral medicine*. 2016;32(3):158-64.
33. Fearon ER. Molecular genetics of colorectal cancer. *Annual review of pathology*. 2011;6:479-507.
34. Armaghany T, Wilson J, Chu Q, Mills G. Genetic alterations in colorectal cancer. *Gastrointestinal cancer research*. 2012;5:19-27.
35. Baker S, Preisinger A, Jessup J, Paraskeva C, Markowitz S. p53 gene mutations occur in combination with 17p allelic deletions as late events in colorectal tumorigenesis. *Cancer research*. 1990;50:7717-22.
36. Perz E, Kuhn J. p53 in the pathogenesis, diagnosis and treatment of cancer. *Journal of oncology pharmacy practice*. 1998;4(2):75-102.
37. Rosrigues N, Rowan A, Smith M, Kerr I, Bodmer W. p53 mutations in colorectal cancer. *Proceedings of the national academy of sciences of the United States of America*. 1990;87:7555-9.
38. Li XL, Zhou J, Chen ZR, Chng WJ. P53 mutations in colorectal cancer - molecular pathogenesis and pharmacological reactivation. *World journal of gastroenterology*. 2015;21(1):84-93.
39. Iacopetta B. TP53 mutation in colorectal cancer. *Human mutation*. 2003;21(3):271-6.
40. Huxley RR, Ansary-Moghaddam A, Clifton P, Czernichow S, Parr CL, Woodward M. The impact of dietary and lifestyle risk factors on risk of colorectal cancer: a quantitative

overview of the epidemiological evidence. *International journal of cancer*. 2009;125(1):171-80.

41. Astin M, Griffin T, Neal RD, Rose P, Hamilton W. The diagnostic value of symptoms for colorectal cancer in primary care: a systematic review. *British journal of general practice*. 2011;61(586):231-43.
42. Greene FL PD, Fleming ID. *AJCC cancer staging system*. 8th ed: Springer; 2017.
43. Kanemitsu Y, Komori K, Kimura K, Kato T. D3 lymph node dissection in right hemicolectomy with a no-touch isolation technique in patients with colon cancer. *Diseases of the colon and rectum*. 2013;56(7):815-24.
44. Kye BH, Cho HM. Overview of radiation therapy for treating rectal cancer. *Annals of coloproctology*. 2014;30(4):165-74.
45. Hafner MF, Debus J. Radiotherapy for colorectal cancer: current standards and future perspectives. *Visceral medicine*. 2016;32(3):172-77.
46. André T, Boni C, Navarro M, Tabernero J, Hickish T, Topham C, et al. Improved overall survival with oxaliplatin, fluorouracil, and leucovorin as adjuvant treatment in stage II or III colon cancer in the MOSAIC trial. *Journal of clinical oncology*. 2009;27(19):3109-16.
47. Pizzorno G, Diasio RB, YC C. *Pyrimidine analogs Holland-Frei cancer medicine*. 6th ed: BC Decker; 2003.
48. Katzung BG, Masters SB, Trevor AJ. *Basic and clinical pharmacology*. 12th ed. New York: McGraw-Hill; 2012.
49. Ali I, Wani WA, Saleem K, Haque A. Platinum compounds: a hope for future cancer chemotherapy. *Anti-cancer agents in medicinal chemistry*. 2013;13(2):296-306.
50. Chay WY, Chew L, Yeoh TT, Tan MH. An association between transient hypokalemia and severe acute oxaliplatin-related toxicity predominantly in women. *Acta oncologica*. 2010;49(4):515-17.
51. Takano M, Sugiyama T. UGT1A1 polymorphisms in cancer: impact on irinotecan treatment. *Pharmacogenomics and personalized medicine*. 2017;10:61-8.
52. Adeeb S, Jaetae L, Tae-Lin H, and Young Sup L. Curcumin induces apoptosis in human colorectal carcinoma (HCT-15) cells by regulating expression of prp4 and p53. *Molecules and cells*. 2013;35(6):526-32.

53. Yogosawa S, Yamada Y, Yasuda S, Sun Q, Takizawa K, Sakai T. Dehydrozingerone, a structural analogue of curcumin, induces cell-cycle arrest at the G2/M phase and accumulates intracellular ROS in HT-29 human colon cancer cells. *Journal of natural products*. 2012;75(12):2088-93.
54. Dinicola S, Marigiò MA, Morabito C, Guarnieri S, Cucina A, Pasqualato A, et al. Grape seed extract triggers apoptosis in Caco-2 human colon cancer cells through reactive oxygen species and calcium increase: extracellular signal-regulated kinase involvement. *British journal of nutrition*. 2013;110(5):797-809.
55. Jin Z, El-Deiry WS. Overview of cell death signaling pathways. *Cancer biology and therapy*. 2014;4(2):147-71.
56. Tait SW, Green DR. Mitochondria and cell death: outer membrane permeabilization and beyond. *Nature reviews molecular cell biology*. 2010;11(9):621-32.
57. Clarke N, Germain P, Altucci L, Gronemeyer H. Retinoids: potential in cancer prevention and therapy. *Expert reviews in molecular medicine*. 2004;6(25):1-23.
58. de Thonel A, Eriksson JE. Regulation of death receptors—relevance in cancer therapies. *Toxicology and applied pharmacology*. 2005;207(2):123-32.
59. Tsujimoto Y. Role of Bcl-2 family proteins in apoptosis: apoptosomes or mitochondria? *Genes to cells*. 2001;3(11):697-707.
60. Dai Y, Grant S. Targeting multiple arms of the apoptotic regulatory machinery. *Cancer research*. 2007;67(7):2908-11.
61. Gustafsson AB, Gottlieb RA. Bcl-2 family members and apoptosis, taken to heart. *American journal of physiology cell physiology*. 2007;292(1):45-51.
62. Lu Z, Xu S. ERK1/2 MAP kinases in cell survival and apoptosis. *IUBMB life*. 2006;58(11):621-31.
63. Fang JY, Richardson BC. The MAPK signalling pathways and colorectal cancer. *The lancet oncology*. 2005;6(5):322-27.
64. Temraz S, Mukherji D, Shamseddine A. Dual inhibition of MEK and PI3K pathway in KRAS and BRAF mutated colorectal cancers. *International journal of molecular sciences*. 2015;16(9):22976-88.
65. Thatcher JD. The RAS-MAPK signal transduction pathway. *Science signaling*. 2010;3(119):1.

66. Meloche S, Pouysségur J. The ERK1/2 mitogen-activated protein kinase pathway as a master regulator of the G1- to S-phase transition. *Oncogene*. 2007;26(22):3227-39.
67. Kidger AM, Siphthorp J, Cook SJ. ERK1/2 inhibitors: new weapons to inhibit the RAS-regulated RAF-MEK1/2-ERK1/2 pathway. *Pharmacology and therapeutics*. 2018;187:45-60.
68. Mochizuki H, Breen M. Comparative aspects of BRAF mutations in canine cancers. *Veterinary sciences*. 2015;2(3):231-45.
69. Bartholomeusz C, Gonzalez-Angulo AM. Targeting the PI3K signaling pathway in cancer therapy. *Expert opinion on therapeutic targets*. 2012;16(1):121-30.
70. Yu M, Grady WM. Therapeutic targeting of the phosphatidylinositol 3-kinase signaling pathway: novel targeted therapies and advances in the treatment of colorectal cancer. *Therapeutic advances in gastroenterology*. 2012;5(5):319-37.
71. Molinari F, Frattini M. Functions and regulation of the PTEN gene in colorectal cancer. *Frontiers in oncology*. 2013;3(326):1-8.
72. Kim HK, Hairani R, Jeong H, Jeong MG, Chavasiri W, Hwang ES. CBMG, a novel derivative of mansonone G suppresses adipocyte differentiation via suppression of PPARgamma activity. *Chemico-biological interactions*. 2017;273:160-70.
73. Tiew P, Ioset J-R, Kokpol U, Schenk K, Jaiboon N, Chaichit N, et al. Four new sesquiterpenoid derivatives from the heartwood of *Mansonia gagei*. *Journal of natural products*. 2002;65(9):1332-35.
74. Pongboonrod S. *Mai Tet Muang Thai*. Bangkok: Amarin printing; 1976.
75. Tiew P, Ioset JR, Kokpol U, Chavasiri W, Hostettmann K. Antifungal, antioxidant and larvicidal activities of compounds isolated from the heartwood of *Mansonia gagei*. *Phytotherapy research*. 2003;17(2):190-93.
76. Smitinand T. *Thai plant names*. Revised ed. Bangkok: Royal forest department; 2014.
77. Eiadthong W. Let's know about Mai-Chan and custom of royal family's funeral. *Journal of forest management*. 2008;2(4):29-45.
78. Tanaka N, Yasue M, Imamura H. The quinonoid pigments of *Mansonia altissima* wood. *Tetrahedron letters*. 1966;7(24):2767-73.

79. Mongkol R, Chavasiri W. Antimicrobial, herbicidal and antifeedant activities of mansonone E from the heartwoods of *Mansonia gagei* Drumm. *Journal of integrative agriculture*. 2016;15(12):2795-802.
80. Kim J-P, Kim W-G, Koshino H, Jung J, Yoo I-D. Sesquiterpene O-naphthoquinones from the root bark of *Ulmus davidiana*. *Phytochemistry*. 1996;43(2):425-30.
81. Soldani C, Lazze MC, Bottone MG, Tognon G, Biggiogera M, Pellicciari CE, et al. Poly(ADP-ribose) polymerase cleavage during apoptosis: when and where? *Experimental cell research*. 2001;269(2):193-201.
82. Simon H-U, Haj-Yehia A, Levi-Schaffer F. Role of reactive oxygen species (ROS) in apoptosis induction. *Apoptosis*. 2000;5(5):415-8.
83. Kim SH, Dass CR. p53-targeted cancer pharmacotherapy: move towards small molecule compounds. *Journal of pharmacy and pharmacology*. 2011;63(5):603-10.
84. Muller PA, Vousden KH. Mutant p53 in cancer: new functions and therapeutic opportunities. *Cancer cell*. 2014;25(3):304-17.
85. Houbiers JG, van der Burg SH, van de Watering LM, Tollenaar RA, Brand A, van de Velde CJ, et al. Antibodies against p53 are associated with poor prognosis of colorectal cancer. *British journal of cancer*. 1995;72(3):637-41.
86. Chaturvedi P, Goka E, Garza ADL, Lopez DM, Lippman ME. Rac1b overexpression confers resistance to chemotherapy treatment in colorectal cancer. *Cancer research*. 2018;78(13):4824.
87. Jensen NF, Stenvang J, Beck MK, Hanakova B, Belling KC, Do KN, et al. Establishment and characterization of models of chemotherapy resistance in colorectal cancer: towards a predictive signature of chemoresistance. *Molecular oncology*. 2015;9(6):1169-85.
88. Seeber A, Gastl G. Targeted therapy of colorectal cancer. *Oncology research and treatment*. 2016;39(12):796-802.
89. de Vries A, Flores ER, Miranda B, Hsieh H-M, van Oostrom CTM, Sage J, et al. Targeted point mutations of p53 lead to dominant-negative inhibition of wild-type p53 function. *Proceedings of the national academy of sciences of the United States of America*. 2002;99(5):2948-53.

90. Kawiak A, Lojkowska E. Ramentaceone, a naphthoquinone derived from *Drosera* sp., induces apoptosis by suppressing PI3K/AKT signaling in breast cancer cells. *PLoS One*. 2016;11(2):1-16.
91. Liu C, Shen GN, Luo YH, Piao XJ, Jiang XY, Meng LQ, et al. Novel 1,4-naphthoquinone derivatives induce apoptosis via ROS-mediated p38/MAPK, Akt and STAT3 signaling in human hepatoma Hep3B cells. *International journal of biochemistry and cell biology*. 2018;96:9-19.
92. Wang JR, Shen GN, Luo YH, Piao XJ, Shen M, Liu C, et al. The compound 2-(naphthalene-2-thio)-5,8-dimethoxy-1,4-naphthoquinone induces apoptosis via reactive oxygen species-regulated mitogen-activated protein kinase, protein kinase B, and signal transducer and activator of transcription 3 signaling in human gastric cancer cells. *Drug development research*. 2018;79(6):1-12.
93. Zhu Y, Zhong Y, Zhou Y, Liu Y, Huang Q, Huang Z, et al. Acetylshikonin inhibits colorectal cancer growth via PI3K/AKT/mTOR signaling pathway. *Chinese medicine*. 2018;9(3):126-43.
94. Li R, Sutphin PD, Schwartz D, Matas D, Almog N, Wolkowicz R, et al. Mutant p53 protein expression interferes with p53-independent apoptotic pathways. *Oncogene*. 1998;16(25):3269-77.
95. Brown JM, Wouters BG. Apoptosis, p53, and tumor cell sensitivity to anticancer agents. *Cancer research*. 1999;59(7):1391-99.
96. Qiu HY, Wang PF, Lin HY, Tang CY, Zhu HL, Yang YH. Naphthoquinones: a continuing source for discovery of therapeutic antineoplastic agents. *Chemical biology and drug design*. 2018;91(3):681-90.
97. Liu B, Chen Y, St Clair DK. ROS and p53: a versatile partnership. *Free radical biology and medicine*. 2008;44(8):1529-35.
98. Macip S, Igarashi M, Berggren P, Yu J, Lee SW, Aaronson SA. Influence of induced reactive oxygen species in p53-mediated cell fate decisions. *Molecular and cellular biology*. 2003;23(23):8576-85.
99. Shapiro GI, Koestner DA, Matranga CB, Rollins BJ. Flavopiridol induces cell cycle arrest and p53-independent apoptosis in non-small cell lung cancer cell lines. *Clinical cancer research*. 1999;5(10):2925-38.

100. Turner J, Abeysinghe RD, Haynes R, Torti SV, Greene BT, Torti FM, et al. p53-independent apoptosis mediated by tachpyridine, an anti-cancer iron chelator. *Carcinogenesis*. 2001;22(10):1607-14.
101. Wang L, Yeung JH, Hu T, Lee WY, Lu L, Zhang L, et al. Dihydratanshinone induces p53-independent but ROS-dependent apoptosis in colon cancer cells. *Life sciences*. 2013;93(8):344-51.
102. Tsang WP, Chau SPY, Kong SK, Fung KP, Kwok TT. Reactive oxygen species mediate doxorubicin induced p53-independent apoptosis. *Life sciences*. 2003;73(16):2047-58.
103. Ye Q, She QB. Integration of AKT and ERK signaling pathways in cancer: biological and therapeutic implications. *Journal of pharmacology and clinical toxicology*. 2013;1(2):1-4.
104. De Luca A, Maiello MR, D'Alessio A, Pergameno M, Normanno N. The RAS/RAF/MEK/ERK and the PI3K/AKT signalling pathways: role in cancer pathogenesis and implications for therapeutic approaches. *Expert opinion on therapeutic targets*. 2012;16:17-27.
105. Wang YK, Zhu YL, Qiu FM, Zhang T, Chen ZG, Zheng S, et al. Activation of AKT and MAPK pathways enhances the tumorigenicity of CD133+ primary colon cancer cells. *Carcinogenesis*. 2010;31(8):1376-80.
106. Meng LQ, Wang Y, Luo YH, Piao XJ, Liu C, Wang Y, et al. Quinalizarin induces apoptosis through reactive oxygen species (ROS)-mediated mitogen-activated protein kinase (MAPK) and signal transducer and activator of transcription 3 (STAT3) signaling pathways in colorectal cancer cells. *Medical science monitor*. 2018;24:3710-19.
107. Cagnol S, Chambard JC. ERK and cell death: mechanisms of ERK-induced cell death--apoptosis, autophagy and senescence. *The journal of FEBS*. 2010;277(1):2-21.
108. Gulati AP, Yang YM, Harter D, Mukhopadhyay A, Aggarwal BB, Benzil DL, et al. Mutant human tumor suppressor p53 modulates the activation of mitogen-activated protein kinase and nuclear factor-kappaB, but not c-Jun N-terminal kinase and activated protein-1. *Molecular carcinogenesis*. 2006;45(1):26-37.
109. Randhawa H, Kibble K, Zeng H, Moyer MP, Reindl KM. Activation of ERK signaling and induction of colon cancer cell death by piperlongumine. *Toxicology in vitro*. 2013;27(6):1626-33.

110. Xiao D, Singh SV. Phenethyl isothiocyanate-induced apoptosis in p53-deficient PC-3 human prostate cancer cell line is mediated by extracellular signal-regulated kinases. *Cancer research*. 2002;62:3615-19.
111. Lin KL, Chien CM, Tseng CH, Chen YL, Chang LS, Lin SR. Furano-1,2-naphthoquinone inhibits Src and PI3K/Akt signaling pathways in Ca9-22 human oral squamous carcinoma cells. *Integrative cancer therapies*. 2014;13(3):18-28.



APPENDIX A
PREPARATION OF REAGENTS

1. DMEM stock solution (1 L)

DMEM powder	10.4 g
NaHCO ₃	3.7 g
ddH ₂ O	900 ml

Adjust pH to 7.4 with 1 N HCl or 1 N NaOH

Add ddH₂O to 1 liter and sterilized by filtering through a 0.2 sterile membrane filter

Store at 4°C

2. RPMI 1640 stock solution (1 L)

RPMI powder	10.4 g
NaHCO ₃	1.5 g
Glucose	4.5 g
Sodium pyruvate	0.11 g
HEPES (1M)	10 ml
ddH ₂ O	900 ml

Adjust pH to 7.2 with 1 N HCl or 1 N NaOH

Add ddH₂O to 1 liter and sterilized by filtering through a 0.2 sterile membrane filter

Store at 4°C

3. DMEM high glucose stock solution (1 L)

DMEM powder	10.4 g
NaHCO ₃	3.7 g
Glucose	4.5 g

ddH ₂ O	900 ml
--------------------	--------

Adjust pH to 7.4 with 1 N HCl or 1 N NaOH

Add ddH₂O to 1 liter and sterilized by filtering through a 0.2 sterile membrane filter

Store at 4°C

4. 1X Phosphate Buffered Saline (PBS) (1 L)

NaCl	8.065 g
------	---------

KCl	0.2 g
-----	-------

KH ₂ PO ₄	0.2 g
---------------------------------	-------

Na ₂ HPO ₄	1.15 g
----------------------------------	--------

ddH ₂ O	900 ml
--------------------	--------

Adjust pH to 7.4 with 1 N HCl or 1 N NaOH

Add ddH₂O to 1 liter and sterilized by autoclaving

Store at room temperature

5. 1X Assay Buffer for Flow Cytometer (100 ml)

HEPES (1M)	1.0 ml
------------	--------

CaCl ₂ (0.1M)	2.8 ml
--------------------------	--------

NaCl (5M)	2.5 ml
-----------	--------

ddH ₂ O	93.7 ml
--------------------	---------

Store at 4°C

6. Hank Buffer Salt Solution (HBSS) (1 L)

Hank balance salt powder	9.8 g
--------------------------	-------

NaHCO ₃	0.35 g
--------------------	--------

ddH ₂ O	850 ml
--------------------	--------

Adjust pH to 7.24 with 1 N HCl or 1 N NaOH

Add ddH₂O to 1 liter and sterilized by filtering through a 0.2 sterile membrane filter

Store at room temperature

7. Separating buffer (500 ml)

Tris base	45.43 g
-----------	---------

ddH ₂ O	350 ml
--------------------	--------

Adjust pH to 8.8 with 1 N HCl or 1 N NaOH

Add ddH₂O to 500 ml

Store at 4°C

8. Stacking buffer (500 ml)

Tris base	15.14 g
-----------	---------

ddH ₂ O	350 ml
--------------------	--------

Adjust pH to 6.8 with 1 N HCl or 1 N NaOH

Add ddH₂O to 500 ml

Store at 4°C

9. Sample diluting buffer (SDB) (225 ml)

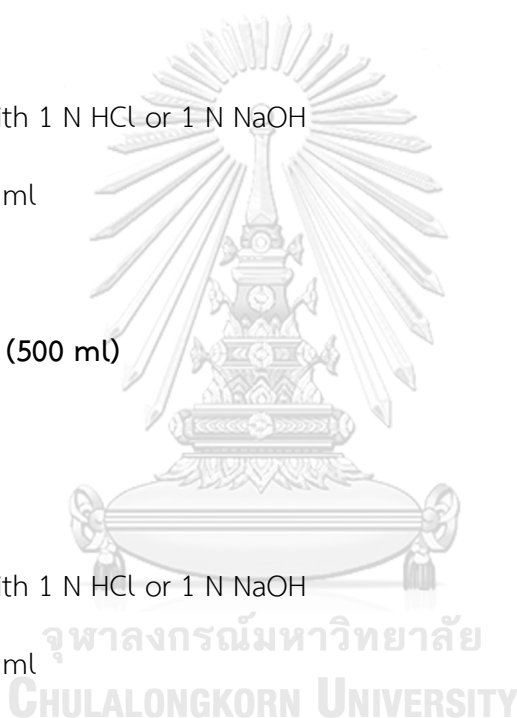
Stacking buffer	31.25 ml
-----------------	----------

10% Sodium dodecyl sulfate (SDS)	50 ml
----------------------------------	-------

Pyronin Y (0.5% stock)	5 ml
------------------------	------

Bromophenol blue (0.5% stock)	5 ml
-------------------------------	------

Glycerol	50 ml
----------	-------



Add ddH₂O to 225 ml

Store at room temperature

10. 10X Leamli buffer (1 L)

Tris base	30.25 g
Glycine	144 g
Sodium dodecyl sulfate (SDS)	10 g
ddH ₂ O	700 ml

Add ddH₂O to 1 liter

Store at 4°C

11. 1X Leamli buffer (1 L)

10X leamli buffer	100 ml
ddH ₂ O	900 ml

Store at 4°C

12. 10X Tris-Buffered Saline (TBS) (1 L)

Tris base	12.1 g
NaCl	87.5 g
ddH ₂ O	800 ml

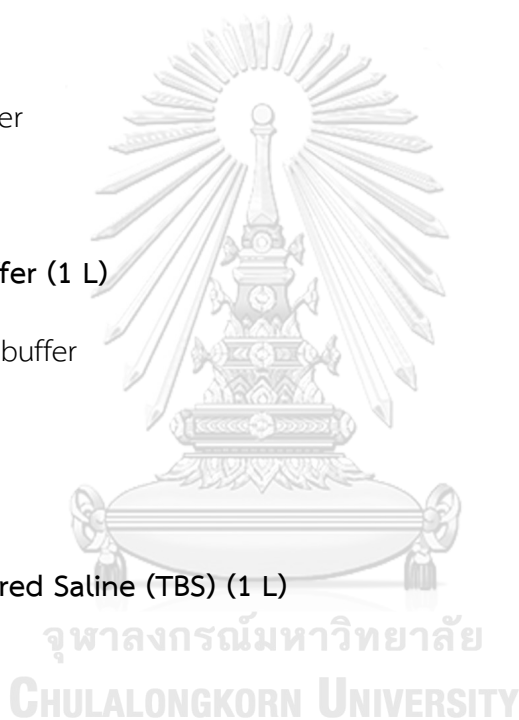
Adjust pH to 7.4 with 1 N HCl or 1 N NaOH

Add ddH₂O to 1 liter

Store at 4°C

13. 1X Tris-Buffered Saline (TBS) (1 L)

10X Tris-Buffered Saline (TBS)	100 ml
--------------------------------	--------



ddH ₂ O	900 ml
--------------------	--------

Store at 4°C

14. 1X Tris-Buffered Saline (TBS)/Tween buffer (1 L)

Tween 20	0.5 ml
----------	--------

Tris-Buffered Saline (TBS)	999.5 ml
----------------------------	----------

Store at 4°C

15. 10X Transfer buffer (1 L)

Tris base	30 g
-----------	------

Glycine	144 g
---------	-------

Sodium dodecyl sulfate (SDS)	1 g
------------------------------	-----

ddH ₂ O	700 ml
--------------------	--------

Add ddH₂O to 1 liter

Store at 4°C

16. 1X Transfer buffer (1 L)

10X Transfer buffer	100 ml
---------------------	--------

methanol	200 ml
----------	--------

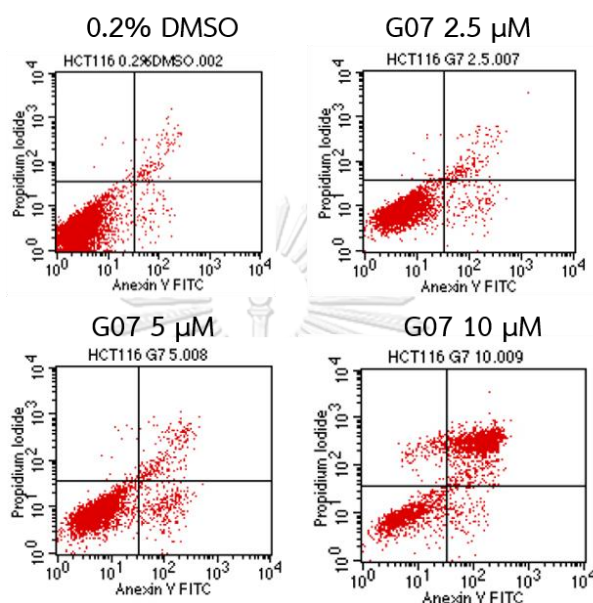
ddH ₂ O	700 ml
--------------------	--------

Store at 4°C

APPENDIX B

RESULTS

Appendix B-1: Representative cytograms of cell apoptosis analysis of HCT-116 cells after treatment with G07 at 2.5, 5 and 10 μM for 24 h.

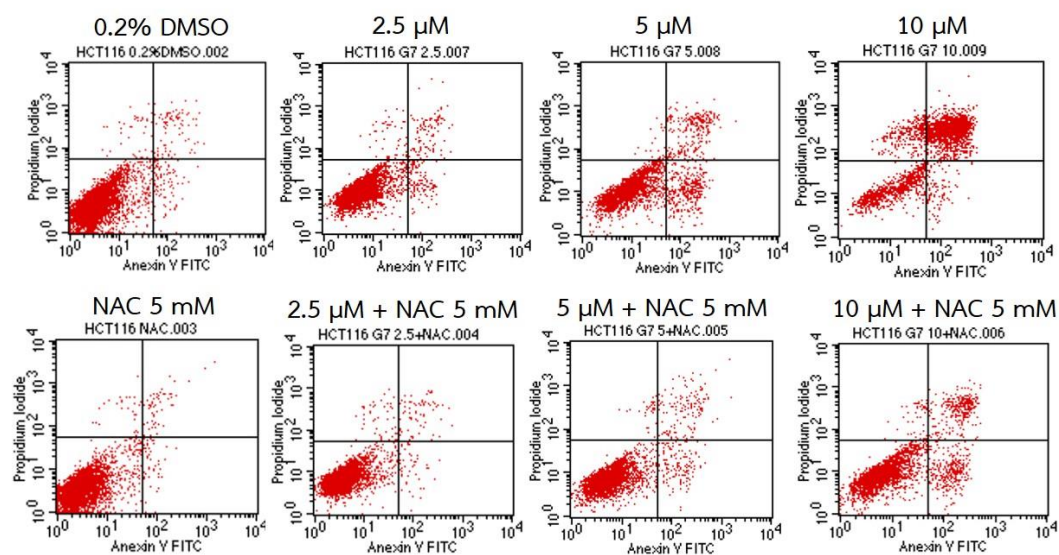


Appendix B-2: The percentages of apoptotic and necrotic cells of HCT-116 cells after treatment with G07 at 2.5, 5 and 10 μM for 24 h.

Treatment	Cell apoptosis (%)			
	Alive	Early apoptosis	Late apoptosis	Necrosis
0.2% DMSO	95.50±1.90	1.11±0.52	2.39±1.17	1.01±0.46
G07 2.5 μM	92.56±1.22	2.18±0.74	3.72±0.75	1.54±0.30
G07 5 μM	83.32±3.88	7.39±2.43	7.91±1.61	1.39±0.43
G07 10 μM	39.06±5.70	4.75±2.57	49.43±7.60	6.77±1.94

Data represent mean±SEM from three independent experiments.

Appendix B-3: Representative cytograms of cell apoptosis analysis of HCT-116 cells after treatment with or without 5 mM of NAC for 1 h and then treated with G07 at 2.5, 5 and 10 μ M for 24 h.



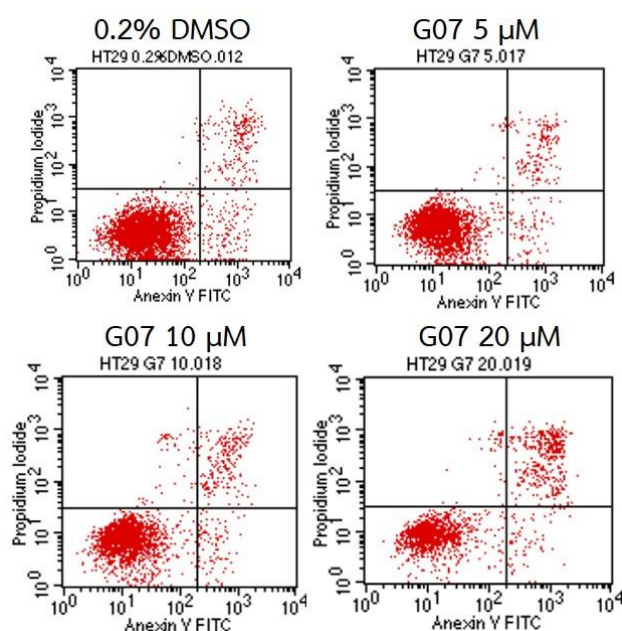
Appendix B-4: The percentages of apoptotic and necrotic cells of HCT-116 cells after treatment with or without 5 mM of NAC for 1 h and then treated with G07 at 2.5, 5 and 10 μ M for 24 h.

Treatment	Cell apoptosis (%)			
	Alive	Early apoptosis	Late apoptosis	Necrosis
0.2% DMSO	94.33±1.00	1.63±0.21	3±0.85	1.04±0.43
NAC 5 mM	94.33±1.64	1.34±0.17	3.09±0.98	1.24±0.66
G07 2.5 μ M	91.43±0.59	3.05±0.43	4.20±0.71	1.32±0.43
G07 5 μ M	81.41±1.99	8.86±1.11	8.50±1.10	1.23±0.48
G07 10 μ M	38.03±5.68	6.19±1.86	47.97±7.14	7.81±0.98
G07 2.5 μ M + NAC 5 mM	93.86±1.47	1.44±0.17	2.96±0.63	1.74±0.87
G07 5 μ M + NAC 5 mM	89.72±0.94	4.53±0.50	4.56±0.85	1.19±0.53

G07 10 μ M + NAC 5 mM	79.91 \pm 1.62	9.23 \pm 0.39	9.38 \pm 1.50	1.47 \pm 0.49
------------------------------	------------------	-----------------	-----------------	-----------------

Data represent mean \pm SEM from three independent experiments.

Appendix B-5: Representative cytograms of cell apoptosis analysis of HT-29 cells after treatment with G07 at 5, 10 and 20 μ M for 24 h.

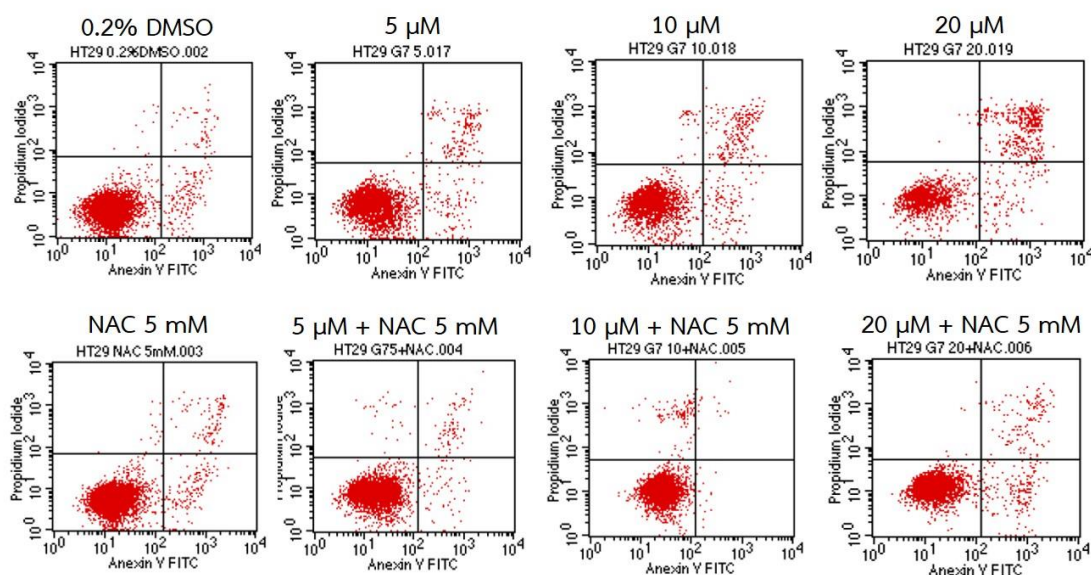


Appendix B-6: The percentages of apoptotic and necrotic cells of HT-29 cells after treatment with G07 at 5, 10 and 20 μ M for 24 h.

Treatment	Cell apoptosis (%)			
	Alive	Early apoptosis	Late apoptosis	Necrosis
0.2% DMSO	91.91 \pm 2.45	3.57 \pm 0.98	4.15 \pm 1.70	0.37 \pm 0.14
G07 5 μ M	90.66 \pm 1.22	4.04 \pm 0.46	4.88 \pm 1.48	0.42 \pm 0.18
G07 10 μ M	87.89 \pm 2.78	3.89 \pm 0.35	6.53 \pm 2.24	1.69 \pm 0.51
G07 20 μ M	66.92 \pm 2.40	6.28 \pm 1.19	24.98 \pm 1.28	1.81 \pm 0.65

Data represent mean \pm SEM from three independent experiments.

Appendix B-7: Representative cytograms of cell apoptosis analysis of HT-29 cells after treatment with or without 5 mM of NAC for 1 h and then treated with G07 at 5, 10 and 20 μ M for 24 h.



Appendix B-8: The percentages of apoptotic and necrotic cells of HT-29 cells after treatment with or without 5 mM of NAC for 1 h and then treated with G07 at 5, 10 and 20 μ M for 24 h.

Treatment	Cell apoptosis (%)			
	Alive	Early apoptosis	Late apoptosis	Necrosis
0.2% DMSO	94.24±2.66	2.89±1.21	2.56±1.56	0.32±0.14
NAC 5 mM	93.99±2.56	2.38±0.65	2.99±1.75	0.64±0.24
G07 5 μ M	92.75±1.99	3.55±0.93	3.37±1.51	0.32±0.08
G07 10 μ M	90.93±2.97	3.54±0.64	4.34±2.25	1.19±0.20
G07 20 μ M	70.36±5.15	6.82±0.71	21.69±4.06	1.13±0.55
G07 5 μ M + NAC 5 mM	92.56±2.34	3.49±0.92	3.28±1.69	0.67±0.14
G07 10 μ M + NAC 5 mM	92.95±2.15	3.08±1.41	2.50±1.63	1.48±0.74

G07 20 μ M + NAC 5 mM	86.45 \pm 2.38	6.80 \pm 0.96	5.86 \pm 1.77	0.88 \pm 0.64
------------------------------	------------------	-----------------	-----------------	-----------------

Data represent mean \pm SEM from three independent experiments.



VITA

NAME Savinee Chanvijit

DATE OF BIRTH 3 April 1993

PLACE OF BIRTH Samutprakan

INSTITUTIONS ATTENDED Bachelor of Science in Microbiology, Chulalongkorn University



จุฬาลงกรณ์มหาวิทยาลัย
CHULALONGKORN UNIVERSITY